PROJECT ADMINISTRATION DATA SHEET

[x] **ORIGINAL**	[ ] **REVISION NO.** _____

Project No. E-21-F09 (R6226-0A0)　　　　　GTRC/~~GIT~~ 　　DATE 10/17/86

Project Director: Atif S. Debs　　　　　　　School/~~Lab~~ Electrical Engineerin

Sponsor: U. S. Department of Energy

Bonneville Power Administration

Type Agreement: Contract No. DE-AI79-86BP65007

Award Period: From 10/1/86 To 9/30/87 (Performance) 9/30/87 (Reports)

Sponsor Amount:

	This Change	Total to Date
Estimated:	$ 62,024	$ 62,024
Funded:	$ 62,024	$ 62,024

Cost Sharing Amount: $ None　　　　　　Cost Sharing No: N/A

Title: Application of the Transient Energy Function Method to the BPA
System

ADMINISTRATIVE DATA　　　　　OCA Contact Brian J. Lindberg x. 4820

1) Sponsor Technical Contact:

James M. Ray - EOX

U. S. Department of Energy

Bonneville Power Administration

P. O. Box 3621

Portland, Oregon 97208

(503) 230-3802

2) Sponsor Admin/Contractual Matters:

Larry Parrish - EMRC

U. S. Department of Energy

Bonneville Power Administration

Lloyd Center Tower, 7th Floor

825 N. E. Multnomah

Portland, Oregon 97232 (503)230-403:

Defense Priority Rating: N/A　　　　Military Security Classification: N/A

　　　　　　　　　　　　(or) Company/Industrial Proprietary: N/A

RESTRICTIONS

See Attached N/A Supplemental Information Sheet for Additional Requirements.

Travel: Foreign travel must have prior approval — Contact OCA in each case. Domestic travel requires sponsor
approval where total will exceed greater of $500 or 125% of approved proposal budget category.

Equipment: Title vests with None proposed or anticipated.

COMMENTS:

SPONSORED PROJECT TERMINATION/CLOSEOUT SHEET

Date___8/30/88_____

Project No.____E-21-F09_____R6226-0A0_____ School/XXX__EE_____

Includes Subproject No.(s)_____N/A_____

Project Director(s)_____Atif S. Debs_____ GTRC/GIT

Sponsor_____U. S. Department of Energy_____

Title_____Application of the Transient Energy Function Method to the BPA System_____

Effective Completion Date:_____9/30/87_____ (Performance)__9/30/87___ (Reports)

Grant/Contract Closeout Actions Remaining:

☐ None

☐ Final Invoice or Copy of Last Invoice Serving as Final   Already submitt[

☒ Release and Assignment

☒ Final Report of Inventions and/or Subcontract:
    Patent and Subcontract Questionnaire
    sent to Project Director ☒

☒ Govt. Property Inventory & Related Certificate

☐ Classified Material Certificate

☐ Other_____

Continues Project No._____ Continued by Project No._____

COPIES TO:

Project Director
Research Administrative Network
Research Property Management
Accounting
Procurement/GTRI Supply Services
Research Security Services
Reports Coordinator (OCA)
Program Administration Division
Contract Support Division   (2)

Facilities Management - ERB
Library
GTRC
Project File
Other _____
     _____
     _____
     _____

TECHNICAL MEMORANDUM 1

THE TEF METHOD WITH CONSTANT CURRENT LOADS

by

A. S. Debs (PI)
School of Electrical Engineering
Georgia Institute of Technology
Atlanta, Georgia 30332-0250

1. INTRODUCTION

In this memorandum, the TEF method is extended to consider constant current loads. The original TEF considers constant impedance loads only. The net outcome of this development is the added flexibility to treat any load as a combination of constant impedance and constant current components. Initially, all loads are assumed to be of the constant current type. Once this problem is resolved, the more general combination case is treated.

2. LOAD FLOW WITH CONSTANT CURRENT LOADS

In order to motivate the discussion, we shall consider a load flow problem where the load is specified to be at a constant current value. Typically, this may occur in a contingency analysis situation where a base-case power flow solution is available for computing the values of the required constant currents. This problem is formulated in terms of the following set of equations:

$$Y_{LL}V_L + Y_{LG}V_G = I_L \tag{1}$$

$$Re\left[Diag\,[V_G]\,[Y_{GL}V_L + Y_{GG}V_G]^*\right] = P_G \,, \tag{2}$$

where the subscripts L and G correspond to load and generation buses, respectively. Furthermore, the following notation/definitions are used:

$$Y \overset{\Delta}{=} \text{Bus Admittance Matrix}$$

$$= \begin{bmatrix} Y_{LL} & Y_{LG} \\ Y_{GL} & Y_{GG} \end{bmatrix}$$

$$\text{Diag}[V_G] = \begin{bmatrix} V_{G_1} & 0 \\ 0 & V_{G_n} \end{bmatrix}$$

I_L = Load Bus Complex Constant Injected Current

$V \overset{\Delta}{=}$ Bus Complex Voltage Vector

$$= \begin{bmatrix} V_L \\ V_G \end{bmatrix}$$

It is to be noted that an equation for the slack bus is not included under the usual assumption of constant voltage magnitude and zero phase angle for that bus.

Since the right hand sides of Eqs. (1) and (2) are specified, one can solve for V_L and V_G by any appropriate algorithm (e.g., Newton-Raphson). In our context, however, we shall carry our variable substitutions in order to eliminate V_L. From Eq. (1), one concludes

$$V_L = Y_{LL}^{-1}[I_L - Y_{LG}V_G] \ . \tag{3}$$

This is then substituted in Eq. (2) to yield

$$P_G = \text{Re}\left[\text{Diag}[V_G]\left[(Y_{GG} - Y_{GL}Y_{LL}^{-1}Y_{LG})V_G + Y_{GL}Y_{LL}^{-1}I_L\right]^*\right] . \tag{4}$$

Defining

$$Y_{eq} = Y_{GG} - Y_{GL}Y_{LL}^{-1}Y_{LG}$$

$$I_{eq} = Y_{GL}Y_{LL}^{-1}I_L ,$$

one concludes

$$P_G = \text{Re}\left[\text{Diag}[V_G][Y_{eq}V_G + I_{eq}]^*\right] \tag{5}$$

Obviously, Y_{eq} is the reduced bus admittance matrix (assuming that the load does not produce an equivalent shunt element), and I_{eq} is a vector of equivalent load current distributed over all generation buses. For a specific generation bus, one expresses (5) as follows:

$$P_{G_i} = V_{G_i}^2 G_{ii} + \sum_{\substack{j=1 \\ j \neq i}}^{n} \left[C_{ij}\sin(\delta_i - \delta_j) + D_{ij}\cos(\delta_i - \delta_j) + V_{G_i}I_{G_i}\cos(\delta_i - \psi_i) \right] , \tag{6}$$

where

n = Number of generators

$V_{G_i} \overset{\Delta}{=} V_{G_i} < \delta_i$

$I_{G_i} \overset{\Delta}{=} I_{G_i} < \psi_i = \text{constant}$

$C_{ij} = V_{G_i}V_{G_j}B_{ij}$

$D_{ij} = V_{G_i}V_{G_j}G_{ij}$

$Y_{eq} = G + jB.$

Without any loss of generality, we let bus G_m be the slack bus. Consequently, Eq. (6) for $i = 1,...,n-1$, together with the slack bus assumption will form the basic set of equations for the new load flow. It differs from the regular load flow in the last term which involves the contribution of the equivalent current.

3. THE SWING EQUATION WITH CONSTANT CURRENT LOADS

The above formulation allows us to write the swing equation as follows:

$$\dot{\delta}_i = \omega_i$$

(7)

$$M_i\dot{\omega}_i = P_{mi} - P_{G_i}$$

where

$$P_{G_i} = V_{G_i}^2 G_{ii} + \sum_{\substack{j=1 \\ j \neq i}}^{m} \left[G_{ij}\sin(\delta_i - \delta_j) + D_{ij}\cos(\delta_i - \delta_j) \right] + V_{G_i} I_{G_i} \cos(\delta_i - \psi_i) \ . \quad (8)$$

Obviously, Eq. (8) is a restatement of Eq. (6), although the context is a bit different, since the generator terminal buses are also reduced in this case. Using standard TEF notation, one rewrites the above equations as:

$$\dot{\delta}_i = \omega_i$$

(7')

$$M_i\dot{\omega}_i = P_i - P_{e_i}$$

where

$$P_i = P_{m_i} - V_{G_i}^2 G_{ii}$$

(8')

$$P_{e_i} = P_{G_i} - V_{G_i}^2 G_{ii}$$

4. THE TRANSIENT ENERGY FUNCTION WITH CONSTANT CURRENT LOADS

The transient energy function (TEF) is defined as:

$$V = \int_{t_s}^{t} \left[\sum_{i=1}^{n} M_i \tilde{\omega}_i - P_i + P_{e_i} + \frac{M_i}{M_T} P_{COI} \right] \dot{\theta}_i dt \; . \tag{9}$$

In the above, the variables chosen revolve around the center of inertia variables (COI) as follows:

$$\delta_o \triangleq \text{center of angle}$$

$$= \frac{1}{M_T} \sum_{i=1}^{n} M_i \delta_i \tag{10}$$

$$M_T = \sum_{i=1}^{n} M_i$$

The motioin of the center of inertia is given by

$$M_T \dot{\omega}_o = \sum_{i=1}^{n} P_i - P_{e_i} \triangleq P_{COI}$$

$$\dot{\delta}_o = \omega_o \tag{11}$$

The generator's motion w.r.t. the COI is given by

$$\theta_i = \delta_i - \delta_o$$

$$\tilde{\omega}_i = \dot{\theta}_i = \omega_i - \omega_o \tag{12}$$

The equations of motion in the COI reference frame are

$$M_i \dot{\tilde{\omega}}_i = P_i - P_{e_i} - \frac{M_i}{M_T} P_{COI}$$

$$\dot{\theta}_i = \tilde{\omega}_i$$

(13)

where P_{e_i} is given by

$$P_{e_i} = \sum_{\substack{j=1 \\ j \neq i}}^{n} \left[C_{ij} \sin(\theta_i - \theta_j) + D_{ij} \cos(\theta_i - \theta_j) \right] + V_{G_i} I_{G_i} \cos(\theta_i + \delta_0 - \psi_i) .$$

(14)

Using established result for the TEF, the new TEF is given by

$$V = \sum_{i=1}^{n} \frac{1}{2} M_i \tilde{\omega}_i^2 - \sum_{i=1}^{n} P_i \left(\theta_i - \theta_i^s \right)$$

$$- \sum_{i=1}^{n} \sum_{j=k+1}^{n} \left\{ C_{ij} \left[\cos(\theta_i - \theta_j) - \cos\left(\theta_i^s - \theta_j^s \right) \right] \right.$$

$$- \int_{\theta_i^s + \theta_j^s}^{\theta_i + \theta_j} D_{ij} \cos(\theta_i - \theta_j) d(\theta_i + \theta_j) \right\}$$

$$+ \sum_{i=1}^{n} \int_{\theta_i^s}^{\theta_i} V_i I_i \cos(\theta_i + \delta_0 - \psi_i) d\theta_i .$$

(15)

The last expression in Eq. (15) represents the contribution of constant current loads to the TEF. Unfortunately, it depends on δ_0, which is the

center of angle of the system. This causes two significant problems: (1) how to evaluate the last integral in Eq. (15), and (2) how this term impacts on the evaluation of the stable and unstable equilibrium points (SEP and UEP, respectively). Our conjecture is that the easiest way out of this dilemma is to hold δ_o at a constant value determined at some appropriate point like at time of fault clearing.

Given the above assumption, the last term in Eq. (15) becomes

$$\sum_{i=1}^{n} \int_{\theta_i^s}^{\theta_i} V_i I_i \cos(\theta_i + \delta_o - \psi_i) d\theta_i$$

$$= \sum_{i=1}^{n} V_i I_i [\sin(\theta_i + \delta_o - \psi_i) - \sin(\theta_i^s + \delta_o - \psi_i)] . \tag{16}$$

5. POST-FAULT SEP AND UEP DETERMINATION

Given the above developments, the load flow equations to be used in computing both the SEP and UEP are given by:

$$P_i = P_{e_i} + \frac{M_i}{M_T} P_{COI} \quad , \quad i = 1,\ldots,n-1$$

$$0 = \sum_{i=1}^{n} M_i \theta_i \tag{17}$$

where P_{e_i} is the same as given in Eq. (14) with δ_o held constant, and

$$P_{COI} = \sum_{i=1}^{n} (P_i - P_{e_i})$$

The standard methods for SEP and UEP computations should hold, with the added proviso that the contribution of the equivalent current should be incorporated. This adds some complexity which should not be too serious, since this last term has only n components, in contrast to the other terms which have n^2 components.

6. CONCLUSION

This technical memorandum provides the conceptual, mathematical, and practical framework for including constant current loads in the TEF program. Success hinges on one approximation that requires δ_o to be held constant at some appropriate value. Validation of this should be attempted through carefully constructed simulations.

GEORGIA INSTITUTE OF TECHNOLOGY
SCHOOL OF ELECTRICAL ENGINEERING
ATLANTA, GEORGIA 30332

ELEPHONE: (404) 894- 2918

May 5, 1987

Mr. Donald Watkins (OGEA)
Bonneville Power Administration
P. O. Box 491
Vancouver, Washington 98666

Dear Don:

Enclosed, please find three (3) copies of Technical Memorandum 2, entitled, "Update of TEF with Constant Current Loads". This is a follow-up on Technical Memorandum 1. Basically, we have resolved all the theoretical obstacles for using a constant current load model within TEF. Presently, we are modifying the EPRI software to test our results.

With best regards,

Sincerely,

/Atif Debs (PI)

ASD/mjc

cc: OCA (Office of Contract Administration)

Project E21-F09

Technical Memorandum 2

UPDATE OF TEF WITH CONSTANT CURRENT LOADS

by

A. S. Debs (PI)
School of Electrical Engineering
Georgia Institute of Technology
Atlanta, Georgia   30332-0250

1. INTRODUCTION

Following up on the development in Technical Memorandum 1, this update resolves the critical difficulty whereby the center of angle $\delta_o(t)$ appears in the various expressions for the transient energy function (TEF) and the special load flow equations. In what follows, we shall describe, step-by-step, how the constant current model is to be employed in the pre-fault, during the fault, and in the post-fault calculations.

2. PRELIMINARIES

For purposes of clarity, we shall denote by the superscripts (1), (2), and (3) the pre-fault, faulted, and post-fault relevant quantities, respectively. Specifically, the interconnection admittance matrix Y will be given by

$$Y^{(k)} = \begin{bmatrix} Y_{LL}^{(k)} & Y_{LG} \\ Y_{GL} & Y_{GG} \end{bmatrix} , \quad k = 1,2,3 \qquad (1)$$

in order to emphasize that a different Y_{LL} matrix is to be dealt with as "k" proceeds from (1) to (3). For a specific load-flow bus i in the pre-fault network, I_i, the corresponding "constant" current is given by

$$I_L = -\frac{(P_i - jQ_i)}{V_i^*}$$

$$= -\frac{(P_i - jQ_i)}{|V_i|^2} V_i$$

where $S_i = P_i + jQ_i$ is the complex load at bus i. Obviously, I_L, the original vector of complex constant currents is

$$I_L = \begin{bmatrix} I_1 \\ \vdots \\ I_m \end{bmatrix} \qquad (2)$$

where m is the number of load-flow busses.

Referring to Technical Memorandum 1 (TM1), we note immediately that there are three distinct equivalent current sources at the internal generator buses. Specifically,

$$I_{eq}^{(k)} = Y_{GL}(Y_{LL}^{(k)})^{-1} I_L \quad , \quad k = 1,2,3 \qquad (3)$$

Furthermore, for the sake of completeness, there are three distinct equivalent interconnection matrices $Y_{eq}^{(k)}$, $k = 1,2,3$, given by:

$$Y_{eq}^{(k)} = Y_{GG} - Y_{GL}(Y_{LL}^{(k)})^{-1} Y_{LG} \quad , \quad k = 1,2,3 \qquad (4)$$

3. PRE-FAULT CALCULATIONS

These are the same as those obtained in the standard stability procedures. Their aim is to determine the internal machine angles $(\delta_1,\ldots,\delta_n)$ and voltages $(E_1,\ldots,E_n)$ at $t = 0^-$.

4. FAULTED NETWORK CALCULATIONS

The main requirement here is to come up with the various acceleration terms $(P_{m_i} - P_{e_i})/M_i$ for the internal generator buses. Now P_{e_i}, the electrical power flowing from the generators "i", is computed on the basis of the <u>faulted network</u> (i.e., $k = 2$). Note

$$P_{e_i}^o = E_i^2 G_{ii}^{(2)} + \sum_{\substack{j=1 \\ j \neq i}}^{n} [C_{ij}^{(2)} \sin(\delta_i^o - \delta_j^o) + D_{ij}^{(2)} \cos(\delta_i^o - \delta_j^o)] + V_i I_i^{(2)} \cos(\delta_i^o - \psi_i^{(2)}) \qquad (5)$$

2

where:

superscript o refers to $t = 0^+$

$$I_i^{(2)} = I_i^{(2)} < \psi_i^{(2)} = \text{equivalent current injections during faulted conditions (i.e., } k = 2)$$

$$C_{ij}^{(2)} = E_i E_j B_{ij}^{(2)}$$

$$D_{ij}^{(2)} = E_i E_j G_{ij}^{(2)}$$

$$Y_{eq}^{(2)} = G^{(2)} + jB^{(2)}$$

Obviously, the acceleration terms (treated as constants in the present TEF procedure) will be given by

$$\frac{d\omega_i}{dt} = \frac{1}{M_i} \left[P_{m_i} - P_{e_i}^o \right] \tag{6}$$

5. POST-FAULT CALCULATIONS

Here is the crux of the problem. It will depend to a great extent on the expression for P_{e_i} in the center of inertia (COI) reference frame. It will be expressed as follows:

$$P_{e_i} = E_i^2 G_{ii}^{(3)} + \sum_{j \neq i} \left[C_{ij}^{(3)} \sin(\theta_i - \theta_j) + D_{ij}^{(3)} \cos(\theta_i - \theta_j) \right]$$

$$+ E_i I_i^{(3)} \cos\left(\theta_i + \delta_o - \psi_i^{(3)} \right) \tag{7}$$

Here, we need to make a critical observation. The equivalent current phase angles $\psi_i^{(3)}$, are, in reality, referenced against the slack bus of the original load flow problem. In the TEF formulation, generator n terminal bus is

3

treated as the slack bus. Let the load-flow bus number of that terminal be ℓ_n. In the load flow case $\delta_{\ell_n} = 0$, by assumption. Had we chosen δ_{ℓ_n} to be any arbitrary angle, then

$$\psi_i^{\,\prime} = \psi_i^{(3)} + \delta_{\ell_n} \qquad\qquad (8)$$

where $\psi_i^{\,\prime}$ is the correct current phase angle in the moving slack bus reference frame. One can assume that as long as the fault is away from the slack bus (a matter that can always be arranged by changing the slack bus), then $\delta_{\ell_n}(t) - \delta_n(t) = \Delta_n \cong$ constant. This means that we can write

$$\delta_o(t) - \psi_i^{(3)} \rightarrow \delta_o(t) - \left(\psi_i^{(3)} + \delta_{\ell_n}\right)$$

$$= \delta_o(t) - \left(\psi_i^{(3)} + \delta_n(t) + \Delta_n\right)$$

$$= \delta_o(t) - \delta_n(t) - \Delta_n - \psi_i^{(3)}$$

$$= -\theta_n - \Delta_n - \psi_i^{(3)} \qquad\qquad (9)$$

Therefore,

$$\cos\left(\theta_i + \delta_o - \psi_i^{(3)}\right) \rightarrow \cos\left(\theta_i - \theta_n - \Delta_n - \psi_i^{(3)}\right)$$

Defining

$$\psi_i = \psi_i^{(3)} + \Delta_n \ , \qquad\qquad (10)$$

one concludes

$$\cos\left(\theta_i + \delta_o - \psi_i^{(3)}\right) = \cos(\theta_i - \theta_n - \psi_i) \qquad\qquad (11)$$

where ψ_i is defined in Eq. (10).

What remains now is the derivation of the relevant load flow equations for computing the stable and unstable equilibrium points (i.e., SEP and UEP, respectively).

5.1 Load Flow Specifications

Dropping the superscript (3) in Eq. (7) (for convenience of notation) and using the result in Eq. (11), one can rewrite Eq. (7) as follows:

$$P_{e_i} = E_i^2 G_{ii} + \sum_{j \neq i} \left[C_{ij} \sin \theta_{ij} + D_{ij} \cos \theta_{ij} \right] + F_i \cos(\theta_i - \theta_n - \psi_i) \tag{12}$$

where $F_i = E_i I_i$.

Defining

$$P_i = P_{m_i} - E_i^2 G_{ii} \tag{13}$$

one can first obtain the expression for P_{COI}

$$
\begin{aligned}
P_{COI} &\triangleq \sum_{i=1}^{n} P_{m_i} - P_{e_i} \\
&= \sum_{i=1}^{n} P_{m_i} - \sum_{i=1}^{n} \left\{ E_i^2 G_{ii} + \sum_{j \neq i} \left[C_{ij} \sin \theta_{ij} + D_{ij} \cos \theta_{ij} \right] \right. \\
&\qquad \left. + \sum_{i=1}^{n} F_i \cos(\theta_i - \theta_n - \psi_i) \right\} \\
&= \sum_{i=1}^{n} P_i - 2 \sum_{i=1}^{n-1} \sum_{j=i+1}^{n} D_{ij} \cos \theta_{ij} \\
&\qquad - \sum_{i=1}^{n} F_i \cos(\theta_i - \theta_n - \psi_i) \; .
\end{aligned}
\tag{14}
$$

where $\theta_{ij} = \theta_i - \theta_j$.

The load-flow equations are now given by:

$$P_i = \sum_{j \neq i} [C_{ij}\sin\theta_{ij} + D_{ij}\cos\theta_{ij}] + F_i\cos(\theta_i - \theta_n - \psi_i) + \frac{M_i}{M_T} P_{COI}$$

$$= \sum_{j \neq i} [C_{ij}\sin\theta_{ij} + D_{ij}\cos\theta_{ij}] + F_i\cos(\theta_i - \theta_n - \psi_i)$$

$$+ \frac{M_i}{M_T} [\sum_{j=1}^{n} P_j - 2\sum_{j=1}^{n-1}\sum_{\ell=j+1}^{n} D_{j\ell}\cos\theta_{j\ell} - \sum_{j=1}^{n} F_j\cos(\theta_j - \theta_n - \psi_j)] ,$$

$$i = 1, \ldots, n-1 \qquad (15)$$

This implies:

$$\left(P_i - \frac{M_i}{M_T}\sum_{i=1}^{n} P_i\right) = \sum_{j \neq i} [C_{ij}\sin\theta_{ij} + D_{ij}\cos\theta_{ij}]$$

$$+ F_i\cos(\theta_i - \theta_n - \psi_i) - 2\left(\frac{M_i}{M_T}\right)\sum_{j=1}^{n-1}\sum_{\ell=j+1}^{n} D_{j\ell}\cos\theta_{j\ell}$$

$$- \left(\frac{M_i}{M_T}\right)\sum_{j=1}^{n} F_j\cos(\theta_j - \theta_n - \psi_j) , \quad i = 1, \ldots, n-1 \qquad (16)$$

The last load flow equation is given by:

$$0 = \sum_{i=1}^{n} M_i\theta_i \qquad (17)$$

The set of equations in (16) and (17) constitute all the required equations for the solution for the SEP and the UEP. It is important, at this state, to

express all the Jacobian terms needed in many solution techniques. Defining P_i' as

$$P_i' = P_i - \frac{M_i}{M_T} \sum_{i=1}^{n} P_i \,, \tag{18}$$

then

$$\frac{\partial P_i'}{\partial \theta_j} = - C_{ij}\cos\theta_{ij} + D_{ij}\sin\theta_{ij}$$

$$- 2\left(\frac{M_i}{M_T}\right) \sum_{\substack{k=1 \\ k \neq j}}^{n} D_{kj}\sin\theta_{kj}$$

$$+ \left(\frac{M_i}{M_T}\right)F_j\sin(\theta_j-\theta_n-\psi_j) \quad , \quad \begin{array}{l} j \neq i \,, \\ i,j \neq n \end{array} \tag{19}$$

$$\frac{\partial P_i'}{\partial \theta_i} = \sum_{j \neq i} (C_{ij}\cos\theta_{ij}-D_{ij}\sin\theta_{ij}) - F_i\sin(\theta_i-\theta_n-\psi_i)$$

$$- 2\frac{M_i}{M_T} \sum_{k \neq i} (D_{ki}\sin\theta_{ki})$$

$$+ \frac{M_i}{M_T} F_i\sin(\theta_i-\theta_n-\psi_i) \quad , \quad i \neq n \tag{20}$$

$$\frac{\partial P_i'}{\partial \theta_n} = - C_{in}\cos\theta_{in} + D_{in}\sin\theta_{in} + F_i\sin(\theta_i-\theta_n-\psi_i)$$

$$- 2\left(\frac{M_i}{M_T}\right) \sum_{k=1}^{n-1} D_{kn}\sin\theta_{kn}$$

$$- \frac{M_i}{M_T} F_n\sin(\theta_i-\theta_n-\psi_i) \quad , \quad i=1,\ldots,n-1 \tag{21}$$

5.2 TEF Specifications

Referring back to the TM1, one notes that the transient energy function is given by

$$V(\theta, \widetilde{\omega}) = \text{K.E.}(\widetilde{\omega}) + \text{P.E.}(\theta) \tag{22}$$

where

$$\text{K.E.}(\widetilde{\omega}) = \frac{1}{2} \sum_{i=1}^{n} M_i \widetilde{\omega}_i^2 \tag{23}$$

$$
\begin{aligned}
\text{P.E.}(\theta) &= -\sum_{i=1}^{n} \int_{\theta_s}^{\theta} \left(P_i - P_{ei} - \frac{M_i}{M_T} P_{COI} \right) d\theta_i \\
&= \sum_{i=1}^{n} - P_i \left(\theta_i - \theta_i^s \right) + \sum_{j=1}^{n} \int_{\theta_s}^{\theta} P_{e_i} d\theta_i \\
&= \sum_{i=1}^{n} - P_i \left(\theta_i - \theta_i^s \right) + \sum_{i=1}^{n} \left[\int_{\theta_s}^{\theta} \left[C_{ij} \sin\theta_{ij} + D_{ij} \cos\theta_{ij} \right] d\theta_i \right. \\
&\quad + \sum_{i=1}^{n} \int_{\theta_s}^{\theta} F_i \cos(\theta_i - \theta_n - \psi_i) d\theta_i \\
&\cong \sum_{i=1}^{n} - P_i \left(\theta_i - \theta_i^s \right) \\
&\quad - \sum_{i=1}^{n-1} \sum_{j=i+1}^{n} C_{ij} \left[\cos\theta_{ij} - \cos\theta_{ij}^s \right] \\
&\quad + \sum_{i=1}^{n} \sum_{j=i+1}^{n} K_{ij} \left[\sin\theta_{ij} - \sin\theta_{ij}^s \right] \\
&\quad + \sum_{i=1}^{n} \int_{\theta_s}^{\theta} F_i \cos(\theta_i - \theta_n - \psi_i) d\theta_i \ .
\end{aligned}
\tag{24}
$$

where

$$K_{ij} = \frac{\theta_i + \theta_j - \left(\theta_i^s + \theta_j^s \right)}{\theta_{ij} - \theta_{ij}^s}$$

In order to evaluate the last term in Eq. (24) we will use the same assumption of a straight line trajectory used to come up with K_{ij} quantities. With this assumption:

$$\int_{\theta_i^s}^{\theta_i} \cos(\theta_i - \theta_n - \psi_i) = \frac{\theta_i - \theta_i^s}{(\theta_i - \theta_i^s) - (\theta_n - \theta_n^s)} \left[\sin(\theta_i - \theta_n - \psi_i) - \sin(\theta_i^s - \theta_n^s - \psi_i) \right]$$

Therefore, the new potential energy expression is given by:

$$P.E.(\theta) = - \sum_{i=1}^{n} P_i(\theta_i - \theta_i^s)$$

$$- \sum_{i=1}^{n-1} \sum_{j=i+1}^{n} C_{ij} \left[\cos\theta_{ij} - \cos\theta_{ij}^s \right]$$

$$+ \sum_{i=1}^{n-1} \sum_{j=i+1}^{n} K_{ij} \left[\sin\theta_{ij} - \sin\theta_{ij}^s \right]$$

$$+ \sum_{i=1}^{n-1} F_i L_i \left[\sin(\theta_{in} - \psi_i) - \sin(\theta_{in}^s - \psi_i) \right]$$

$$+ \left(\theta_n - \theta_n^s \right) F_n \cos\psi_n$$

where

$$L_i = \frac{\theta_i - \theta_i^s}{(\theta_i - \theta_i^s) - (\theta_n - \theta_n^s)}$$

6. CONCLUSION

This memorandum provides the proper framework for the treatment of constant current loads. It is based on the reduction procedure established in TM1. It resolves the dilemma of the phase angle of the equivalent current sources. A full specification of the load flow equations and the transient energy function is provided.

Implementation on the standard TEF package requires the following important changes:

1. Calculation of I_L : the complex constant current vector.

2. Performances of network reduction to obtain $I_{eq}^{(2)}$ for the evaluation of initial accelerations during the fault.

3. Evaluation of $I_{eq}^{(3)}$ for the post-fault network and Δ_n that adjusts the angles $\psi_i^{(3)}$.

4. Modification of the expression for computing the mismatch vector in the load flow program.

5. Modifications for the expression for computing the new Jacobian terms.

6. Modifications for including the extra terms in the potential energy expression.

June 9, 1987

Mr. Donald Watkins (OGEA)
Bonneville Power Administration
P. O. Box 491
Vancouver, Washington 98666

Dear Don:

Enclosed, please find three (3) copies of Technical Memorandum 3 entitled, "An Efficient Formulation of the Transient Energy Function Method". In this formulation, very efficient algorithms have been introduced. Preliminary results are excellent.

With best regards,

Sincerely

Atif Debs (PI)

ASD/mjc

Enclosures

cc: OCA (Office of Contract Admin.)

PROJECT E21-F09

TECHNICAL MEMORANDUM 3

AN EFFICIENT FORMULATION

OF THE

TRANSIENT ENERGY FUNCTION METHOD

by

A. S. Debs
School of Electrical Engineering
Georgia Institute of Technology
Atlanta, Georgia   30332-0250

1. SUMMARY

In this memorandum, the following is accomplished:

(1) Equations are derived for solving the post fault stable and unstable equilibrium points without the need for network reduction. This will allow the use of sparse matrix techniques like in a regular load flow approach.

(2) The derivations in (1) are extended to the case of constant current loads together with constant impedance loads.

(3) Evaluation of the "magnetic energy" term in the potential energy function is reduced from evaluating $\frac{n(n-1)}{2}$ terms, to n terms, where n = no. of generators.

(4) Other terms in the P.E. function are shown to depend strictly on the reduced conductance matrix G. This reduction step seems unavoidable.

(5) The method of computing the P.E. function is extended to the case of constant current loads.

2. POST FAULT SOLUTION METHODS

In the original reference frame the swing equations were given by

$$\dot{\delta}_i = \omega_i$$

$$M_i \frac{d\omega_i}{dt} = P_{mi} - P_{ei}$$

(1)

where

$$P_{ei} = \frac{V_i V_{ti}}{x'_{di}} \sin(\delta_i - \delta_{ti})$$

(2)

V_i = internal voltage magnitude at generator i

δ_i = internal voltage angle at generator i

V_{ti} = terminal voltage magnitude at generator i

δ_{ti} = terminal voltage angle at generator i

i = 1,...,n = no. of generators.

Defining the complex vectors:

$\underline{V}_L$ = vector of complex voltages at all network buses including gener-
ator terminal buses (but not internal ones)

$\underline{V}_G$ = vector of complex internal generator voltages.

Assuming constant impedance loads $\underline{V}_L$, $\underline{V}_G$, are related by the relation

$$\underline{Y}_{LL} \, \underline{V}_L + \underline{Y}_{LG} \, \underline{V}_G = 0 \tag{3}$$

where $\underline{Y}_{LL}$ is the admittance matrix (including loads represented as constant admittances) restricted to network buses. $\underline{Y}_{LG}$ corresponds to the interconnection matrix between terminal to and internal generator buses.

If one is interested in the post-fault steady state solution, the following steps are followed:

(1) Select one bus as the slack bus. For convenience one my choose the last generator bus to be the slack bus. In this case, $\delta_n = 0$.

(2) Solve, by means of an appropriate algorithm, the following set of equations:

$$P_{mi} = \frac{V_i V_{ti}}{x'_{di}} \sin(\delta_i - \delta_{ti}) \quad , \quad i = 1,...,n-1$$

$$\underline{Y}_{LL} \, \underline{V}_L + \underline{Y}_{LG} \, V_G = 0$$

2

Normally, one would use an iterative scheme like the Newton-Raphson method. This can be quite efficient since the resulting Jacobian will be very sparse (load flow sparsity level). In the center of inertia (COI) reference frame, the angles δ_i become

$$\delta_i = \theta_i + \delta_o$$

where

$$\delta_o = \frac{1}{M_T} \sum_{i=1}^{n} M_i \delta_i$$

$$M_T = \sum_{i=1}^{n} M_i$$

The resulting equations to be solved are:

$$P_{mi} = P_{ei} + \frac{M_i}{M_T} P_{COI} \quad , \quad i = 1,\ldots,n$$

(5)

$$0 = \underline{Y}_{LL} \, \tilde{\underline{V}}_L + \underline{Y}_{LA} \, \tilde{\underline{V}}_G$$

where $\dfrac{P_{COI}}{M_T}$ represents the acceleration of the center of inertia of the system. In (5) above, we have made the following transformation

$$\tilde{\underline{V}}_L = \underline{V}_L e^{-j\delta_o}$$

$$\tilde{\underline{V}}_G = \underline{V}_G e^{-j\delta_o}$$

so that

$$P_{ei} = \frac{V_i V_{ti}}{x'_{di}} \sin(\theta_i - \theta_{it})$$

3

In essence, all phase angles in the network are shifted by δ_o radians. Since P_{COI} depends on all generator angles, the first set of equations in (5) is not sparse at all. However, we note the following: Each one of those equations can be written as:

$$\frac{M_T}{M_i} P_{m_i} = \frac{M_T}{M_i} P_{ei} + P_{COI} \tag{6}$$

which implies:

$$\frac{M_T}{M_i} P_{m_i} - \frac{M_T}{M_{i+1}} P_{m_{i+1}} = \frac{M_T}{M_i} P_{ei} - \frac{M_T}{M_i} P_{e_{i+1}} \tag{7}$$

$$\text{for} \quad i = 1,\ldots,n-1 \ .$$

The equations in (7) are sparse indeed, containing only four angle variables in each equation. Thus, effectively, the following set of equations need to be solved:

$$\frac{P_{m_i}}{M_i} - \frac{P_{m_{i+1}}}{M_i} = \frac{P_{ei}}{M_i} - \frac{P_{ei+1}}{M_{i+1}} \quad , \quad i = 1,\ldots,n-1 \tag{8}$$

$$\underline{Y}_{LL} \ \tilde{\underline{V}}_G + \underline{Y}_{LG} \ \tilde{\underline{V}}_G = 0$$

plus the relation

$$\sum_{i=1}^{n} M_i \theta_i = 0 \tag{9}$$

The last relation introduces a fairly full row in the Jacobian. In order to avoid this difficulty, we go back to the slack bus concept. Here, we solve Eqs. (8) for the angles $\gamma_1,\ldots,\gamma_n$, such that $\gamma_n = 0$. Then we compute

$$\gamma_o = \frac{1}{M_T} \sum_{i=1}^{n} \gamma_i M_i \tag{10}$$

Consequently,

$$\theta_i = \gamma_i - \gamma_o \tag{11}$$

4

The angles γ_i, $i = 1,...,n$ obey Eqs. (8) with $\gamma_n = 0$. The resulting θ_i's will also obey equations (8) plus (9). The reason is that Eqs. (8) are invariant under a uniform phase shift of all voltage variables.

The above procedure produces a powerful formulation of the problem for computing both the stable and unstable equilibrium points. It has basically the same sparsity structure of a load flow problem with some minor adjustments to accommodate the first set of equations in (8) above. This formulation is less cumbersome than the one proposed in the EPRI workshop in Toronto (May 1986).

3. ENERGY FUNCTION EVALUATION

The potential energy function in TEF is given by

$$V_{P.E.} = -\sum_{i=1}^{n} P_i\left(\theta_i - \theta_i^S\right)$$

$$-\sum_{i=1}^{n-1}\sum_{j=i+1}^{n} C_{ij}\left[\cos\theta_{ij} - \cos\theta_{ij}^S\right]$$

$$+\sum_{i=1}^{n-1}\sum_{j=i+1}^{n} K_{ij}D_{ij}\left[\sin\theta_{ij} - \sin\theta_{ij}^S\right] \tag{12}$$

where

$$P_i = P_{m_i} - V_i^2 G_{ii} \tag{13}$$

$$C_{ij} = V_i V_j B_{ij} \tag{14}$$

$$D_{ij} = V_i V_j G_{ij} \tag{15}$$

$$K_{ij} = \frac{\theta_i + \theta_j - \left(\theta_i^S + \theta_j^S\right)}{\theta_{ij}\theta_{ij}^S} \tag{16}$$

5

$$\theta_{ij} = \theta_i - \theta_j \qquad (17)$$

and where,

$$\underline{Y} = G + jB \qquad (18)$$

is the reduced admittance matrix of the system. We shall proceed by analyzing each of these terms individually:

(1) The term

$$\alpha = \sum_{i=1}^{n-1} \sum_{j=i+1}^{n} C_{ij} \cos\theta_{ij}$$

is given by:

$$\alpha = \sum_{i=1}^{n-1} \sum_{j=i+1}^{n} C_{ij} \cos\theta_{ij}$$

$$= \frac{1}{2} \sum_{i=1}^{n} \sum_{j=1}^{n} V_i V_j B_{ij} \cos(\theta_i - \theta_j) - \frac{1}{2} \sum_{i=1}^{n} V_i^2 B_{ii}$$

$$= \frac{1}{2} \sum_{i,j=1}^{n} V_i V_j B_{ij} [\cos\theta_i \cos\theta_j + \sin\theta_i \sin\theta_j] - \frac{1}{2} \sum_{i=1}^{n} V_i^2 B_{ii}$$

$$= \frac{1}{2} \sum_{i,j} B_{ij} [E_i E_j + F_i F_j] - \frac{1}{2} \sum_{i=1}^{n} V_i^2 B_{ii}$$

$$= \frac{1}{2} E^T B E + \frac{1}{2} F^T B F - \frac{1}{2} \sum_i V_i^2 B_{ii} \qquad (19)$$

where

$$\underline{V}_i = E_i + jF_i$$

$$E = \begin{bmatrix} E_1 \\ \vdots \\ E_n \end{bmatrix} \quad , \quad F = \begin{bmatrix} F_1 \\ \vdots \\ F_n \end{bmatrix} . \qquad (20)$$

At this point, one needs to look for means to evaluate the final expression in Eq. (19). Specifically we are interested in the first two terms, since the last term will eventually cancel out.

One notes that the network equations obey the relations:

$$\begin{bmatrix} \underline{Y}_{LL} & \underline{Y}_{LG} \\ \underline{Y}_{GL} & \underline{Y}_{GG} \end{bmatrix} \begin{bmatrix} \underline{V}_L \\ \underline{V}_G \end{bmatrix} = \begin{bmatrix} 0 \\ \underline{I}_g \end{bmatrix} \tag{21}$$

where $\underline{I}_g$ is the vector of current injections at the internal machine buses. Premultiplying both sides by $\begin{bmatrix} \underline{V}_L^T & \underline{V}_G^T \end{bmatrix}^*$, one obtains:

$$\begin{bmatrix} \underline{V}_L^T & \underline{V}_G^T \end{bmatrix}^* \begin{bmatrix} \underline{Y}_{LL} & \underline{Y}_{LG} \\ \underline{Y}_{GL} & \underline{Y}_{GG} \end{bmatrix} \begin{bmatrix} \underline{V}_L \\ \underline{V}_G \end{bmatrix} = \begin{bmatrix} \underline{V}_L^T & \underline{V}_G^T \end{bmatrix}^* \begin{bmatrix} 0 \\ I_G \end{bmatrix} \tag{22}$$

This is decomposed into the following terms:

$$\begin{bmatrix} \underline{V}_L^T & \underline{V}_G^T \end{bmatrix}^* \begin{bmatrix} \underline{Y}_{LL} \underline{V}_L + \underline{Y}_{LG} \underline{V}_G \\ \underline{Y}_{GL} \underline{V}_L + \underline{Y}_{GG} V_G \end{bmatrix} = V_G^{T*} I_G \tag{23}$$

$$= V_G^{T*} \begin{bmatrix} \underline{Y}_{GL} \underline{V}_L + \underline{Y}_{GG} V_G \end{bmatrix} \tag{24}$$

Now, since

$$\underline{Y}_{LL} \underline{V}_L + \underline{Y}_{LG} \underline{V}_G = 0 \tag{25}$$

then

$$V_L = -\underline{Y}_{LL}^{-1} \begin{bmatrix} \underline{Y}_{LG} \underline{V}_G \end{bmatrix} . \tag{26}$$

Furthermore,

$$(\underline{V}_G^T)^* \underline{I}_G = (\underline{V}_G^T)^* \begin{bmatrix} \underline{Y}_{GG} - \underline{Y}_{GL} \underline{Y}_{LL}^{-1} Y_{LG} \end{bmatrix} V_G \tag{27}$$

But the matrix

$$\underline{Y}_{GG} - \underline{Y}_{GL} \underline{Y}_{LL}^{-1} Y_{LG} \tag{28}$$

7

is exactly the reduced matrix

$$\underline{Y} = G + jB \tag{29}$$

that connects the internal generator buses. Expanding in terms of rectangular coordinates, one obtains

$$\left(\underline{v}_G^T\right)^* \underline{I}_G = \left(E^T - jF^T\right)\left(I_R + jI_I\right)$$

$$= \left(E^T I_R + F^T I_I\right) + j\left(E^T I_I - F^T I_R\right)$$

$$= \left(\underline{v}_G^T\right)^*(G + jB)\underline{v}_G$$

$$= \left(E^T - jF^T\right)(G + jB)\left(E + jF\right)$$

$$= \left(E^T - jF^T\right)\left((GE-BF) + j(BE+GF)\right)$$

$$= E^T GE - E^T BF + F^T BE + F^T GF + j\left(E^T BE + E^T GF - F^T GE + F^T BF\right)$$

$$= E^T GE + F^T GF + j\left(E^T BE + F^T BF\right) \tag{30}$$

Therefore,

$$E^T BE + F^T BF = E^T I_I - F^T I_R \tag{31}$$

The implication then is that

8

$$\alpha - \alpha^S = \sum_{i=1}^{n-1} \sum_{j=i+1}^{n} C_{ij}[\cos\theta_{ij} - \cos\theta_{ij}^S]$$

$$= \frac{1}{2} \left[E^T BE + F^T BF - \sum_{i=1}^{n} V_i^2 B_{ii} \right]$$

$$- \frac{1}{2} \left[(E^S)^T BE^S + (F^S)^T BF^S - \sum_{i=1}^{n} V_i^2 B_{ii} \right]$$

$$= \frac{1}{2} \left[(E^T I_I - F^T I_R) - ((E^S)^T I_I - (F^S)^T I_R^S) \right] \qquad (32)$$

Computationally, one evaluates the internal bus injected currents using the simple formula:

$$\underline{I}_i = (\underline{V}_i - \underline{V}_{ti})(\frac{-j}{x_{di}'})$$

$$= \left[(E_i - E_{ti}) + j(F_i - F_{ti}) \right]\left[\frac{-j}{x_{di}'}\right]$$

$$= \left(\frac{F_i - F_{ti}}{x_{di}'}\right) - j\frac{(E_i - E_{ti})}{x_{di}'} \qquad (33)$$

As a result,

$$\alpha - \alpha^S = \frac{1}{2} \sum_{i=1}^{n} \left[-E_i \frac{(E_i - E_{ti})}{x_{di}'} - \frac{F_i(F_i - F_{ti})}{x_{di}'} \right.$$

$$\left. + \frac{E_i^S(E_i^S - E_{ti}^S)}{x_{di}'} + \frac{F_i^S(F_i^S - F_{ti}^S)}{x_{di}'} \right]$$

$$= \frac{1}{2} \sum_{i=1}^{n} \frac{1}{x_{di}'} \left[E_i^S(E_i^S - E_{ti}^S) - E_i(E_i - E_{ti}) \right.$$

$$\left. + F_i^S(F_i^S - F_{ti}^S) - F_i(F_i - F_{ti}) \right]$$

$$= \frac{1}{2} \sum_{i=1}^{n} \left[(E_i^S)^2 + (F_i^S)^2 - (E_i^2 + F_i^2) \right.$$

$$\left. - (E_i^S E_{ti}^S - E_i E_{ti} + F_i^S F_{ti}^S - F_i F_{ti}) \right] \frac{1}{x_{di}'}$$

$$= \frac{1}{2} \sum_{i=1}^{n} \left[(V_i^S)^2 - (V_i)^2 + (E_i E_{ti} - E_i^S E_{ti}^S + F_i F_{ti} - F_i^S F_{ti}^S) \right] \frac{1}{x_{di}'}$$

$$= \frac{1}{2} \sum_{i=1}^{n} \frac{1}{x_{di}'} \left[E_i E_{ti} - E_i^S E_{ti}^S + F_i F_{ti} - F_i^S F_{ti}^S \right] \tag{34}$$

$$= \frac{1}{2} \sum_{i=1}^{n} \left[\frac{V_i V_{it} (\cos\theta_i' - \theta_{tt}')}{x_{di}'} - \frac{V_i V_{it} \cos(\theta_i^S - \theta_{ti}^S)}{x_{di}'} \right] \tag{35}$$

Thus the evaluation of the term A reduces to a simple summation of n terms.

(2) The term $\quad \beta = \sum_{i=1}^{n-1} \sum_{j=i+1}^{n} K_{ij} D_{ij} \left[\sin\theta_{ij} - \sin\theta_{ij}^S \right]$

may be expressed as

$$\beta = \sum_{i=1}^{n-1} \sum_{j=i+1}^{n} K_{ij} G_{ij} V_i V_j \left[\left(\sin\theta_i \cos\theta_j - \cos\theta_i \sin\theta_j \right) \right.$$

$$\left. - \left(\sin\theta_i^S \cos\theta_j^S - \cos\theta_i^S \sin\theta_j^S \right) \right]$$

$$= \sum_{i=1}^{n-1} \sum_{j=i+1}^{n} K_{ij} G_{ij} \left[(F_i E_j - E_i F_j) - (F_i^S E_j^S - E_i^S F_j^S) \right] \tag{36}$$

Because the term K_{ij} multiplies the conductance term G_{ij}, one cannot use the results of the previous section effectively. The form shown in Eq. (36) is the most efficient computationally in computing β.

10

(3) The term $\gamma = \sum\limits_{i=1}^{n} P_i\left(\theta_i - \theta_i^s\right)$

$$= \sum_{i=1}^{n} P_{m_i}\left(\theta_i - \theta_i^s\right) - \sum_{i=1}^{n} G_{ii} V_i^2\left(\theta_i - \theta_i^s\right) \qquad (37)$$

requires knowledge of the diagonal terms of the G matrix.

In conclusion, the computation of the potential energy function has been simplified as follows:

(a) The "magnetic energy" term involving the susceptance matrix B (α - α^s in the discussion above) was reduced from a complex evaluation of $\frac{n(n-1)}{2}$ terms to that of only n terms. For n = 200, this is a reduction from 10,000 computations to 200, i.e., a 50-fold reduction in computer time and storage.

(b) Evaluation of the other terms require knowledge of the reduced G matrix only. Computations are simplified by converting all voltage quantities to the rectangular coordinate system.

4. CONSIDERATIONS OF CONSTANT CURRENT LOADS - LOAD FLOW EQUATIONS

Let $\underline{I}_L$ define the complex vector of constant current loads. Using the logic of section (b) above, the post-fault steady state equations are:

$$P_{m_i} = \frac{V_i V_{ti}}{x'_{di}} \sin\left(\delta_i - \delta_{ti}\right) \quad , \quad i = 1,\ldots,n$$

$$\tag{38}$$

$$\underline{Y}_{LL} \, \underline{V}_L + \underline{Y}_{LG} \, \underline{V}_G = \underline{I}_L$$

11

where in these equations, the original slack bus retained as the terminal bus of the slack machine. As we move to the COI reference frame, we make _two_ phase angle adjustments. In the first adjustment, the _internal_ slack bus angle is set to zero. And in the second, we move to the COI reference frame. Letting machine n be the slack bus, we note that in (38)

$$\delta_{tn} = 0 \tag{39}$$

Let δ_n^o = initial (prefault) value of δ_n.

As we move the slack bus to the internal slack bus, all network angles are changed to

$$\gamma_i = \delta_i - \delta_n^o \tag{40}$$

Thus in the "γ" reference frame, Eqs. (38) become:

$$P_{mi} = \frac{V_i V_{ti}}{x'_{di}} \sin(\gamma_i - \gamma_{ti}) \quad , \quad i = 1, \ldots, n \tag{41}$$

$$\underline{Y}_{LL} \, \tilde{\underline{V}}_L + \underline{Y}_{LG} \, \tilde{\underline{V}}_G = \underline{I}_L e^{-j\delta_n^o}$$

where

$$\tilde{\underline{V}}_L = \underline{V}_L e^{-j\delta_n^o}$$

$$\tag{42}$$

$$\tilde{\underline{V}}_G = \underline{V}_G e^{-j\delta_n^o}$$

As we move to the COI reference frame, the initial set of equations become:

$$\frac{P_{m_i}}{M_i} + \frac{P_{m_{i+1}}}{M_{i+1}} = \frac{V_i V_{ti}}{x'_{di} M_i} \sin(\gamma_i - \gamma_{ti}) - \frac{V_{i+1} V_{ti+1}}{x'_{di+1} M_{i+1}} \sin(\gamma_{i+1} - \gamma_{ti+1}) \quad ,$$

12

$$i = 1, \ldots, n-1 \tag{43}$$

$$\underline{Y}_{LL} \, \tilde{V}_L + \underline{Y}_{LG} \, \tilde{V}_G = I_L e^{-j\delta_n^o}$$

Having solved for the "γ" variables, the "θ" variables are obtained as in section (b), i.e., by defining

$$\gamma_o = \frac{1}{M_T} \sum_{i=1}^{n} \gamma_i M_i \, , \tag{44}$$

and then concluding that

$$\theta_i = \gamma_i - \gamma_o \tag{45}$$

5. THE POTENTIAL ENERGY FUNCTION WITH CONSTANT CURRENT LOADS

As shown in Technical Memorandum 2, the potential energy function in the presence of constant current loads is given by

$$
\begin{aligned}
V_{P.E.} = &- \sum_{i=1}^{n} \left[P_{m_i} \left(\theta_i - \theta_i^S \right) - V_i^2 G_{ii} \left(\theta_i - \theta_i^S \right) \right] \\
&- \sum_{i=1}^{n-1} \sum_{j=i+1}^{n} C_{ij} \left(\cos\theta_{ij} - \cos\theta_{ij}^S \right) \\
&+ \sum_{i=1}^{n-1} \sum_{j=i+1}^{n} K_{ij} D_{ij} \left(\sin\theta_{ij} - \sin\theta_{ij}^S \right) \\
&+ \sum_{i=1}^{n-1} F_i L_i \left[\sin(\theta_i - \theta_n - \psi_i) - \sin\left(\theta_i^S - \theta_n^S - \psi_i \right) \right] \\
&+ \left(\theta_n - \theta_n^S \right) F_n \cos\psi_n
\end{aligned}
\tag{46}
$$

where

$$L_i = \frac{\theta_i - \theta_i^s}{\left(\theta_i - \theta_i^s\right) - \left(\theta_n - \theta_n^s\right)}$$

$$F_i = V_i I_{eq_i}$$

ψ_i = angle of $\underline{I}_{eq}$ relative to slack internal bus

$$\underline{I}_{eq} = -\underline{Y}_{GL}\, \underline{Y}_{LL}^{-1}\, \underline{I}_L e^{-j\delta_n^o}$$

$\underline{Y}_{LL}$ = post-fault admittance matrix restricted to all but internal generator nodes.

In computing the term

$$A = \sum_{i=1}^{n-1} \sum_{j=i+1}^{n} C_{ij}\left(\cos\theta_{ij} - \cos\theta_{ij}^s\right) \tag{47}$$

As outlined earlier, we note that the relevant network equations are

$$\begin{bmatrix} \underline{Y}_{LL} & \underline{Y}_{LG} \\ \underline{Y}_{GL} & \underline{Y}_{GG} \end{bmatrix} \begin{bmatrix} \tilde{\underline{V}}_L \\ \tilde{\underline{V}}_g \end{bmatrix} = \begin{bmatrix} \underline{I}_L' \\ \underline{I}_g \end{bmatrix} \tag{48}$$

which mean that the equivalent current injections at the generator internal buses are:

$$\underline{I}_g' = \underline{I}_g - \underline{Y}_{GL}\, \underline{Y}_{LL}^{-1}\, \overline{\underline{I}_L'} \tag{49}$$

where

$$\underline{I}_L' = \left(\underline{I}_L e^{-j\delta_n^o}\right) e^{-j\gamma_o} \tag{50}$$

i.e., the equivalent current phase angle is shifted by the same amount as all other voltage angles. Letting

14

$$\underline{I}'_g = I_R - jI_I \tag{51}$$

one can use Eq. (31) to evaluate A as given in Eq. (47).

FINAL REPORT

Submitted to

The U.S. Department of Energy
Bonneville Power Administration
Portland, Oregon

FEASIBILITY OF THE TEF DIRECT STABILITY

METHOD TO THE BPA SYSTEM

VOLUME I - TECHNICAL REPORT

CONTRACT: DE-AI79-86-BP65007

by

School of Electrical Engineering
Georgia Institute of Technology
Atlanta, Georgia 30332-0250

FINAL REPORT

Submitted to

The U.S. Department of Energy
Bonneville Power Administration
Portland, Oregon

FEASIBILITY OF THE TEF DIRECT STABILITY
METHOD TO THE BPA SYSTEM

by

School of Electrical Engineering
Georgia Institute of Technology
Atlanta, Georgia   30332-0250

Principal Investigator   Faculty/Staff   Students

   A. S. Debs   J. Dorsey   I. Belmona
             .   T. Godart
                                                       N. Tisdale

   Consultant

   A. Fouad

TABLE OF CONTENTS
(Continued)

1. EXECUTIVE SUMMARY

1.1 Major Findings

The project was able to provide the following assessments of the feasibility of the Transient Energy Function (TEF) method to the BPA system.

(1) Advantages:

    (a) Computational CPU times of TEF will range from a factor of 3 up to 20 times to speed of comparable time domain simulation analysis program.

    (b) The "energy margins" and associated indices provide the user with a good measure of stability for a given case. In this respect, a single TEF run will summarize information obtainable from several time domain simulation runs.

    (c) The "Mode of Disturbance" (MOD) concept provides another insight into the problem which is hard to identify in the time domain simulation approach.

    (d) The TEF methodology is sufficiently general to incorporate flexible load models, and the effects of DC lines and excitation systems.

    (e) Key issues associated with voltage dip at maximum swing, line apparent impedances, also at maximum swing, and multiple switching sequences, can be accommodated in the overall methodology.

    (f) The use of coherency based reduced order models can be accommodated through the sparse matrix formulation of the TEF method.

1

(2) <u>Disadvantages</u>:

    (a) Although the incorporation of various models into the TEF method is possible, every new step in modeling complexity requires a considerable effort at the analytical end. At some point, there may be some insurmountable barriers beyond which the picture is quite vague at present. For example, issues of multiple swing stability, and more complex machine models are quite illusive at present.

    (b) In stressed systems, there is a strong need for robust laod flow computational techniques to guarantee numerical convergence to correct solutions. This tends to diminish the computational advantage stated earlier.

1.2 Approach

In order to come up with the above findings, the project team was not satisfied with the mere exercise of reviewing past and on-going efforts; or the stated expert opinions of the project consultant. Basically, the sponsor had demanded answers to an extremely challenging set of questions. For example, no known methodology was available for addressing the load modeling, voltage dip, and other problems. Evaluations with available software were not conclusive precisely because of the sponsor's needs.

Consequently, the project team undertook to develop the STEF software package in order to be able to test the feasibility of various issues. This package has been able to answer some of the key questions related to computational efficiency, load modeling, voltage dip, and coherency based dynamic reduction. At the analytical level, these issues were studied with the sparse

formulation of the TEF method. As a result, the information gained from the consultant, past, and on-going efforts, was integrated with the experience of an alternative formulation. By so doing, the findings were finely tuned to better address the needs of the sponsor.

2. PROJECT DEVELOPMENTS

2.1 BPA's Needs

The project is focused on responding to specific needs expressed by BPA staff, initial project proposal, and during joint project meetings. In summary, BPA's needs extend beyond the standard EPRI Direct Stability Method Program capabilities. Specifically, the priority issues for BPA are:

(1) Representation of bus loads as combinations of constant power, current, and impedance.

(2) Identification of low post-disturbance voltages to check if any voltage limit violations will occur.

(3) Modeling of excitation systems and computation, as a result, of the corresponding stability energy margins.

(4) Accounting for the presence of DC lines in the network.

(5) Prediction of post-disturbance energy margins following a sequence of switching operations which may include:

(a) Standard line switchings

(b) Capacitor insertion

(c) Generator dropping

(d) DC line switching.

(6) Prediction of actions by out-of-step relaying systems.

(7) Examining the role of dynamic system reduction in all of the above concerns.

Inherent in the above needs is the key question: How far can the TEF method go to duplicate and improve upon present time domain simulation capabilities?

2.2 Approach

The approach taken by the project staff consisted of the following steps:

(1) Review of all prior accomplishments in direct stability methods.

(2) Detailed review of accomplishments in the EPRI project including work already in progress.

(3) Detailed assessment of the experimental level DIRECT software package developed by Ontario Hydro for TEF stability analysis.

(4) Identification of needed developments to answer BPA's needs.

(5) Evaluation of key concepts using the independently developed STEF software package, and the Dynamic Network Reduction package.

(6) Technical feasibility assessment of BPA's needs.

(7) Definition of needed research and development activities to prove all relevant concepts.

(8) Definition of the structure of a future TEF package for system operations.

(9) Definition of a comparable software structure for system planning.

2.3 Prior and Related Works

Appendix B consists of a report prepared by Professor A. Fouad, as part of the present effort. In it he provides a concise overview of accomplishments, past, underway, and future in the TEF direct stability method. Specifically, we cite the following:

(1) TEF has been tested with a variety of networks and systems, ranging from a few to ≈ 150 generator systems. Its reliability level is in the 95% range. It has worked with plant and inter-area modes of disturbances. Confidence in TEF has led to follow-up activities with a major project with Ontario Hydro.

5

(2) The modeling and preliminary testing of the following has been accomplished:

   (a) DC line models (Appendix C)

   (b) Exciter models (Appendix D)

   (c) Out-of-step relay models (Ref. [15]).

(3) The energy stability margin concept has proven to be effective in assessing the "degree of stability." When used either directly, and/or in the context of sensitivity analysis, it can provide the operator (and planner) guidance and new insights not experienced before.

(4) Attempts to include more detailed machine dynamics have not been made, and most probably, may not prove to be cost effective.

(5) The methodology is limited to first swing stability. There is a potential for studying multiple-swing stability, but this is not called for, at present, or in the near future.

(6) The issue of load modeling, and the prediction of network voltage conditions are yet to be developed. The theory of "structure preserving models" [7] may prove to be very useful.

(7) Application of TEF to large-scale networks will require the avoidance of network reduction approaches, and the use of sparse matrix methods.

2.4 EPRI TEF Package

The project team experimented with an experimental version of the TEF Package provided by Ontario Hydro with EPRI's approval. The package did perform adequately with the sample networks provided. However, it was limited to the following:

(1) The models used consisted of classical generator models and constant impedance loads.

(2) Only the manual "mode of disturbance" option was operational. The automatic option was not.

(3) The code was dimensioned for ≈ 300 generators. From private communications, we learned that networks of up to 230 generators were actually tested. This is less than the 380 generator case for the WSCC system.

(4) It accepts IEEE and PTI data formats and not those of WSCC.

(5) Documentation was not sufficient for making major modifications.

On the positive side, it had the important capabilities to solve for the post-disturbance Stable and Unstable Equilibrium Points (SEP and UEP, respectively), with the aid of a variety of options like the Scaled Newton Raphson (SNR) method, Corrected Gauss-Newton (CGN) method, and others.

From the perspective of BPA's needs, a more advanced package was needed to answer some of the key questions.

2.5 Needed Developments

Based on the above factors, it became clear that the key to answering BPA's needs lies in three closely related developments. These are:

(1) Development of new formulations of the TEF methodologies to account for the sparse nature of the network with its full nonlinear load flow equations, nonlinear load models, and DC line models.

(2) Re-examination of the transient energy expression with specific reference to the potential energy term in light of the nonlinear load models and the need to make computations of this term much more efficient.

7

(3)   Linking of the dynamic reduction program to the TEF program.

Given the earlier and ongoing developments under the EPRI project, and the ones just cited, one can carefully test the practical feasibility of the overall methodolgy for BPA's purposes. This will be illustrated later in the report.

2.6 Actual Developments

In order to meet BPA's expressed needs, it became necessary to carry out extra developmental work. Theoretical formulations may have sufficed for the purposes of a feasibility study. Without developmental work, however, the key issues of practicality, solution convergence, and degrees of approximation could not be adequately assessed.

As a result, we undertook to develop the package STEF (Sparse Analysis of the Transient Energy Function method). Figure 1 provides a general block diagram representation of STEF. It contains three basic options:

Option 0: Load Flow Analysis

This option is used for initial verification of supplied load flow data cases. Invariably, truncation of parameter and solution data creates unacceptable mismatches. These may cause solution inaccuracies in later stability analysis computations.

Option 1: Time Domain Analysis

In this option, the machines are modeled as classical ones. Since TEF uses classical models also, this option provides immediate verification of any results. Presently, this option provides output records for angles of selected machines. It can be easily upgraded to provide voltage information as well.
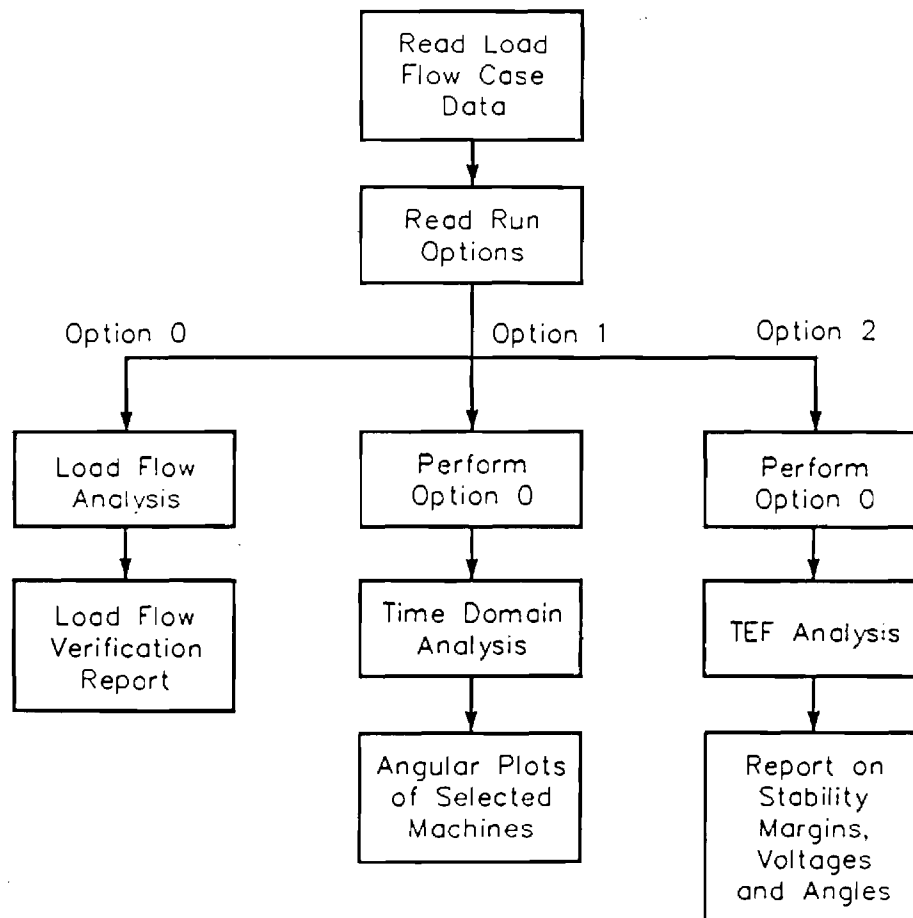
8

Fig. (1):   Block Diagram Representation of the STEF Package

Option 2:   TEF Analysis

This contains the crux of our developments.   It was designed for the analysis of large scale networks using standard stability program load models. It is configured as an experimental "test facility" to allow the study of a variety of issues.   Because of its importance, the next section is devoted to a more detailed description of this option.

The capabilities resulting from the development of STEF will allow the following studies to be performed:

(1) Stability energy margin indices can be obtained for any 3-phase fault followed by a sequence of switching operations for fault clearance and stability enhancement.

(2) Sensitivities of energy margins to fault clearing time, line and generator loadings, and generator/load dropping schemes can be all attained.

(3) Since loads can be represented as combinations of constant impedance, current, and power, then sensitivities to load model coefficients can be easily obtained.

(4) DC lines can be handled in theory, given the proviso described later in this report.   This is possible because of the developed load modeling capabilities.   (Effectively, as shown in Appendix C and Ref. [16], in the post-disturbance period, DC line terminals are modeled as equivalent constant power loads.)

(5) Easy interfacing with the dynamic reduction program.   This is facilitated by the fact that the sparse network formulation will allow the use of phase shifting transformers which result from the aggregation of several machines.

10

There are, however, some limitations which need to be addressed, like:

(1) The present SEP and UEP solution routines use the standard Newton-Raphson solution method. Upgrading these to the Scaled Newton-Raphson (SNR) and Corrected Gauss-Newton (CGN) methods, solution convergence is attainable in more complex situations.

(2) Excitation system models are yet to be implemented and tested.

(3) Interactive user-friendly options are needed for effective use.

2.7 TEF Option Structure

TEF option (Option 2 in the previous section) is summarized in Figure 2. In reference to that figure, the following is noted:

(1) Load model parameters consist of three coefficients, A, B, and C, where:

A = fraction of constant admittance load

B = fraction of constant current load

C = fraction of constant power load

with the proviso that

A + B + C = 1.

In a future program update, individual bus load coefficients can be specified. Furthermore, one may choose a different set of coefficients for real and reactive load at the same bus.

(2) There are four option selections associated with solution methods. The _first_ option selection allows the user to choose the standard network reduction approach for evaluating the dissipation potential energy term whenever the chosen load model is also the standard constant impedance one. Alternatively, the Structure Preserving

11

```
┌─────────────────────┐          ┌─────────────────────┐
│   Specify Load      │          │     Report on       │
│ Model Parameters    │◄────────►│    Load Model       │
│  Solution Method    │          │     and all         │
│     Options         │          │     Options         │
└─────────────────────┘          └─────────────────────┘
           │
           ▼
┌─────────────────────┐          ┌─────────────────────┐
│  Calculate Initial  │          │                     │
│  Machine Voltages   │◄────────►│      Initial        │
│    and Angles       │          │    Conditions       │
│                     │          │      Report         │
└─────────────────────┘          └─────────────────────┘
           │
           ▼
┌─────────────────────┐          ┌─────────────────────┐
│  Calculate Angles   │          │                     │
│  and Voltages at    │◄────────►│     Clearing        │
│   Final Clearing    │          │      Time           │
│       Time          │          │     Report          │
└─────────────────────┘          └─────────────────────┘
           │
           ▼
┌─────────────────────┐          ┌─────────────────────┐
│     Solve for       │◄────────►│  Stable Equilibrium │
│       SEP           │          │    Point Report     │
└─────────────────────┘          └─────────────────────┘
           │
           ▼
┌─────────────────────┐          ┌─────────────────────┐
│     Mode of         │          │   Mode Analysis     │
│   Disturbance       │◄────────►│   and Selection     │
│     Analysis        │          │      Report         │
└─────────────────────┘          └─────────────────────┘
           │
           ▼
┌─────────────────────┐          ┌─────────────────────┐
│    Solve for UEP    │◄────────►│     UEP Report      │
└─────────────────────┘          └─────────────────────┘
           │
           ▼
┌─────────────────────┐          ┌─────────────────────┐
│     Stability       │◄────────►│     Stability       │
│  Margin Analysis    │          │   Margin Report     │
└─────────────────────┘          └─────────────────────┘
```
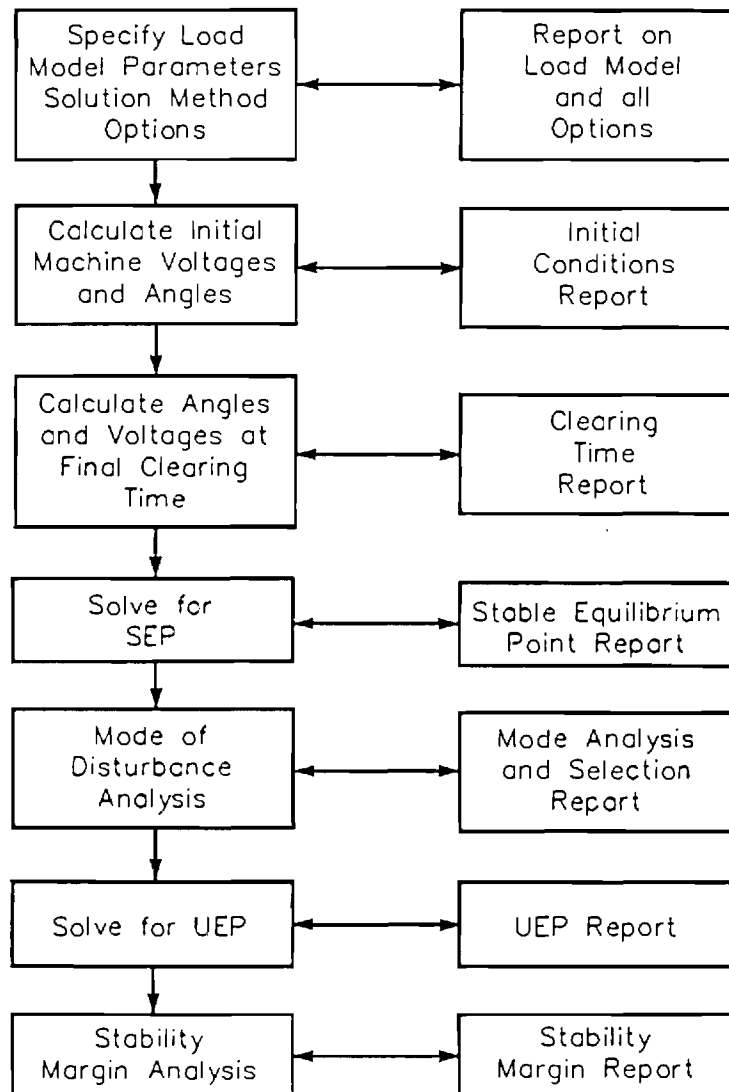
Fig. (2):   Structure of the TEF Option in STEF

Model (SPM) option is used for any load model specified. Obviously, SPM should be automatically specified whenever the load model is not strictly constant impedance type.

In the second option selection, the user can specify if he wants the program to compute the exact UEP solution or the one that maximizes potential energy along the so-called "Ray Line" [2]. In case of solution nonconvergence in the exact option, the program will automatically provide the ray line maximization approximation.

In the third option selection, the user can choose between an exact and an approximate computation of the dissipation potential energy term. There are significant computer CPU time savings associated with the approximate option.

Finally, the fourth option allows the user to either permit an automatic or manual mode of disturbance selection. In the manual case, he can specify any number of MOD's that look plausible.

The remaining blocks in Figure 2 are quite obvious. The mathematical basis for our formulations are discussed later.

2.8 Summary

In summary, in approaching the project tasks and expressed BPA's needs, all prior and ongoing activities were carefully studied and assessed. This helped tremendously in identifying needed activities to attempt to address all the remaining issues. As a result, we were in a much better position to address the feasibility of TEF to the BPA system.

3. TECHNICAL BACKGROUND

3.1 General

This chapter provides a concise background on the technical aspects associated with the TEF method, including the modeling requirements of BPA. It starts with the classical TEF formulation and solution methods, then moves to the sparse formulation with the "Structure Preserving Model." From that, discussion of the critical issues of DC line, exciter, and out-of-step relay models follows. This is then followed by a discussion of dynamic reduction.

3.2 Classical TEF Formulation

In the classical TEF formulation, one assumes:

(1) Classical generator dynamic model of constant voltage behind transient reactance, and

(2) Constant impedance loads.

Letting n_g be the number of generators, we define:

$$\underline{V}_G \overset{\Delta}{=} \text{internal generator complex voltage vector, such that}$$

$$\underline{V}_{Gi} \overset{\Delta}{=} V_{Gi} < \delta_{Gi} \quad , \quad i = 1, \ldots, n_g$$

$$\underline{Y}_{GG} \overset{\Delta}{=} \text{post-disturbance reduced admittance matrix}$$

$$\overset{\Delta}{=} \underline{G} + j\underline{B}$$

$$\omega_{Gi} \overset{\Delta}{=} \text{angular speed of generator } i \; .$$

14

The Center of Inertia (COI) angles and speeds are defined as:

$$\theta_{Gi} = \delta_{Gi} - \delta_o \tag{1}$$

$$\tilde{\omega}_{Gi} = \omega_{Gi} - \omega_o \tag{2}$$

where

$$\delta_o = \frac{1}{M_T} \sum_{i=1}^{n_g} M_{Gi} \delta_{Gi} \tag{3}$$

$$\omega_o = \frac{1}{M_T} \sum_{i=1}^{n_g} M_{Gi} \omega_{Gi} \tag{4}$$

$$M_T = \sum_{i=1}^{n_g} M_{Gi} \tag{5}$$

In the COI reference frame, the swing equations become:

$$M_{Gi} \frac{d\tilde{\omega}_{Gi}}{dt} = P_{m_i} - P_{e_i} - \frac{M_{Gi}}{M_T} P_{COI}$$

$$= P_{m_i} - V_{Gi}^2 G_{ii} - \sum_{\substack{j=1 \\ j \neq i}}^{n_g} V_{Gi} V_{Gj} \left(G_{ij} \cos(\delta_{Gi} - \delta_{Gj}) + B_{ij} \sin(\delta_{Gi} - \delta_{Gj}) \right)$$

$$- \frac{M_{Gi}}{M_T} P_{COI} \tag{6}$$

for $i = 1, \ldots, n_g$, where P_{COI} is given by

$$P_{COI} = \sum_{i=1}^{n_g} (P_{m_i} - P_{e_i}) \ .$$ (7)

P_{m_i} is the constant input mechanical power and P_{e_i} is the electric power output of generator Gi.

The transient energy function is given by

$$V(\widetilde{\omega}, \theta) = V_{KE} + V_{PE}$$ (8)

where

$$V_{KE} = \text{kinetic energy component}$$

$$= \frac{1}{2} \sum_{i=1}^{n_g} M_{Gi} (\widetilde{\omega}_{Gi})^2 \ ,$$ (9)

and

$$V_{PE}(\theta, \theta^S) = \sum_{i=1}^{n_g} \left(-P_{m_i} + V_{Gi}^2 G_{ii} \right) \left(\theta_i - \theta_i^S \right)$$

$$- \sum_{i=1}^{n_g-1} \sum_{j=i+1}^{n_g} V_{Gi} V_{Gj} B_{ij} \left(\cos\theta_{ij} - \cos\theta_{ij}^S \right)$$

$$+ \sum_{i=1}^{n_g-1} \sum_{j=i+1}^{n_g} I_{ij} \ ,$$ (10)

where

θ^S = vector θ at the Stable Equilibrium Point (SEP)

$$\theta_{ij} = \theta_{Gi} - \theta_{Gj} \tag{11}$$

$$I_{ij} = V_{Gi}V_{Gj}G_{ij} \frac{\theta_{Gi} + \theta_{Gj} - \theta_{Gi}^S - \theta_{Gj}^S}{\theta_{ij} - \theta_{ij}^S}\left(\sin\theta_{ij} - \sin\theta_{ij}^S\right) \tag{12}$$

The first summation term is known as the "position energy," the second as the "magnetic energy," and the last as the "dissipation energy."

The minimum of $V_{PE}(\theta,\theta^S)$ is attained at $\theta = \theta^S$, i.e., at SEP. For a given disturbance, the "θ" trajectory will reach a maximum point, at which the potential energy will be at its highest and the kinetic energy zero. The maximum attainable V_{PE} along the given disturbance trajectory will occur at the so-called "Relevant Unstable Equilibrium Point," and it occurs at an extremum of $V_{PE}(\theta,\theta^S)$. Since θ^S occurs at the minimum of $V_{PE}(\theta^S)$, the set of equations used for solving for SEP and UEP is the same. The difference lies in the <u>initial starting solution</u>.

SEP and UEP equations are given by:

$$
\begin{aligned}
P_{m_i} &= P_{e_i} + \frac{M_i}{M_T} P_{COI} \\[2mm]
&= V_{Gi}^2 G_{ii} + \sum_{\substack{j=1 \\ j \neq i}}^{n_g} V_{Gi}V_{Gj}\left[G_{ij}\cos\theta_{ij} + B_{ij}\sin\theta_{ij}\right] \\[2mm]
&\quad + \frac{M_i}{M_T} P_{COI} \quad, \quad i = 1,\ldots n_{g-1}
\end{aligned} \tag{13}
$$

$$\sum_{i=1}^{n_g} P_{m_i} = P_{COI} + \sum_{i=1}^{n_g} P_{e_i}$$

$$= P_{COI} + \sum_{i=1}^{n_g} \sum_{j=1}^{n_g} V_{Gi} V_{Gj} \left[G_{ij} \cos\theta_{ij} + B_{ij} \sin\theta_{ij} \right] \tag{14}$$

$$\sum_{i=1}^{n_g} M_{Gi} \theta_{Gi} = 0 . \tag{15}$$

These are $n_g + 1$ equations to solve for the variables $\theta_{Gi}, \ldots, \theta_{Gn}$ and P_{COI}.

In order to obtain the SEP solution, one can use the prefault internal angles shifted to the COI reference frame as the initial guess. For the UEP solution, the issue is more complex.

Effectively there are many possible UEP solutions $(2^{n_g} - 1)$. The main contribution of recent research is to establish rules for detecting the "controlling UEP solution" by identifying the correct "Mode of Disturbance" (MOD). The correct MOD is defined as that mode where "corrected normalized potential energy margin" is the least among all possible MODs.

Reference [3] defines the procedure for computing the "corrected kinetic energy" as that responsible for system separation. The corrected normalized potential energy margin, ΔV_{PE}^n, is given by:

$$\Delta V_{PE}^n = V_{PE}(\theta^u, \theta^c)/V_{KE,corr} \tag{16}$$

Thus, among all possible MODs, the one with the lowest ΔV_{PE}^n corresponds to the correct MOD.

Once the correct MOD is identified, a good initial UEP solution can be obtained. That solution is then used to obtain the exact UEP solution by means of an iterative algorithm.

18

Experience in the EPRI—Ontario Hydro project has shown that a standard Newton—Raphson algorithm will exhibit divergent behavior in some situations. The Scaled Newton—Raphson (SNR) and Corrected Gauss—Newton (CGN) methods exhibit better convergence properties. In essence, certain MODs correspond to fairly ill-conditioned Jacobian matrices which require more specialized solution techniques.

Defining θ^u to be the solution at the UEP, then the following indices are defined:

(1) Energy Margin

$$\Delta V = V_{PE}(\theta^u, \theta^C) - V_{KE} \tag{17}$$

(2) Corrected Energy Margin

$$\Delta V_{corr} = V_{PE}(\theta^u, \theta^C) - V_{KE,corr} \tag{18}$$

(3) Normalized Energy Margin

$$\Delta V^n = \Delta V / V_{KE} \tag{19}$$

(4) Normalized Corrected Energy Margin

$$\Delta V^n_{corr} = \Delta V_{corr} / V_{KE,corr} \tag{20}$$

Basically, stability is easily determined according to the sign of the corrected energy margin: positive for stable, and negative for unstable. The

19

magnitude of the normalized corrected energy margin will signify the degree of stability (or instability). Its sensitivity to system variables and/or parameters may be used in various decision functions like limits on line loadings, generator loadings, among others.

3.3 Sparse Matrix Formulation

The sparse matrix formulation influences the choice of the set of equations used for SEP and UEP solutions, as well as, the computation of the potential energy function. The net effect is a significant improvement in solution CPU time requirements [17].

(1) Solution Equations. SEP and UEP solution equations for the main network are:

$$\underline{Y}_{LL}\underline{V}_L + \underline{Y}_{LG}\underline{V}_G = 0 \tag{21}$$

where the overall admittance matrix (including internal generator nodes) is:

$$\underline{Y} = \begin{bmatrix} \underline{Y}_{LL} & \underline{Y}_{LG} \\ \underline{Y}_{GL} & \underline{Y}_{GG} \end{bmatrix} \tag{22}$$

and

$\underline{V}_L$ = vector of all complex bus voltages except for internal generator ones.

Furthermore, in the $\underline{Y}_{LL}$ matrix, the equivalent constant impedance loads are already accounted for. This should explain the zero in the right-hand side of Eq. (21).

The internal generator equations can now be simplified as:

20

$$P_{m_i} = P_{e_i} + \frac{M_{Gi}}{M_T} P_{COI}$$

$$= \frac{V_{Gi} V_{ti}}{x'_{di}} \sin(\theta_{Gi} - \theta_{ti}) + \frac{M_i}{M_T} P_{COI} \quad , \quad i = 1,\ldots,n_g - 1 \tag{23}$$

where V_{ti} and θ_{ti} are the voltage magnitude and angle of the terminal bus of generator Gi. The two remaining equations are:

$$\sum_{i=1}^{n_g} P_{m_i} = P_{COI} + \sum_{i=1}^{n_g} P_{e_i}$$

$$= P_{COI} + \sum_{i=1}^{n_g} \frac{V_{Gi} V_{ti}}{x'_{di}} \sin(\theta_{Gi} - \theta_{ti}) \tag{24}$$

and

$$\sum_{i=1}^{n_g} M_{Gi} \theta_{Gi} = 0 \tag{25}$$

With the exception of the last two equations, we have very sparse sets of equations associated with the network and the internal buses. The last equation can be accommodated indirectly by solving all the other equations, with respect to a slack bus reference and then shifting the resulting solution phase angles by the amount δ_o to obtain θ angles which obey Eq. (25). This means that the only "dense" equation, Eq. (24), which is numbered normally at the bottom.

The resulting storage requirements for the Table of Factors are greater than those of the corresponding load flow by the amount of ΔS, where

$$\Delta S < 2(n_g + n_\ell)$$

where n_g is the number of generators and n_ℓ is the number of network buses. For a 2000 bus, 400 generator system:

$$\Delta S < 2(2400) = 4800$$

(2) <u>Potential Energy Function</u>. From the previous section, we identified the potential "magnetic" energy term as:

$$V_{PE(m)} = - \sum_{i=1}^{n_g-1} \sum_{j=i+1}^{n_g} V_{Gi} V_{Gj} B_{ij} \left(\cos\theta_{ij} - \theta_{ij}^S \right) \tag{26}$$

With little mathematical manipulation, one can show that:

$$V_{PE(m)} = - \frac{1}{2} \sum_{i=1}^{n_g} \frac{V_{Gi} V_{ti}}{x_{di}'} \left(\cos(\theta_{Gi} - \theta_{ti}) - \cos(\theta_{Gi}^S - \theta_{ti}^S) \right) \tag{27}$$

Thus, instead of evaluating $\frac{n_g(n_g-1)}{2}$ terms, we evaluate a similar set of n_g terms. Note that the magnetic potential energy term is nothing more than the sum of differences of injected reactive power at internal generator nodes from θ to θ^S (times 0.5).

The dissipation energy term is a bit more complicated. This term is given by:

$$V_{PE(\theta,\theta^S)} = \sum_{i=1}^{n_g-1} \sum_{j=i+1}^{n_g} V_{Gi} V_{Gj} G_{ij} \frac{\theta_{Gi} + \theta_{Gj} - \theta_{Gi}^S - \theta_{Gj}^S}{\theta_{ij} - \theta_{ij}^S} \left(\sin\theta_{ij} - \sin\theta_{ij}^S \right)$$

$$= \sum_{i=1}^{n_g-1} \sum_{j=i+1}^{n_g} V_{Gi} V_{Gj} G_{ij} K_{ij} \tag{28}$$

22

Now if θ_{ij} and θ_{ij}^S are small in magnitude, then $\sin\theta_{ij} - \sin\theta_{ij}^S \cong \theta_{ij} - \theta_{ij}^S$. If this is true for all $i,j = 1,\ldots,n_g$, then the above expression is approximated by

$$V_{PE(d)} \simeq \sum_{i=1}^{n_g} \left(\sum_{j=1}^{n_g} V_{Gi} V_{Gj} G_{ij} \right) \left(\theta_{Gi} - \theta_{Gi}^S \right)$$

$$\triangleq \sum_{i=1}^{n_g} g_{Gi} \left(\theta_{Gi} - \theta_{Gj}^S \right) \tag{29}$$

where,

$$g_{Gi} \triangleq \sum_{\substack{j=1 \\ j \neq i}}^{n_g} V_{Gi} V_{Gj} G_{ij} . \tag{30}$$

Now, if θ_{Gi} corresponds to an "advanced" machine, then $(\theta_{Gi} - \theta_{Gj})$ is not necessarily small in magnitude. This means we cannot use the above approximation for that machine. By restricting the above approximation to the "non-advanced" machines only, one obtains:

$$V_{PE(\theta,\theta^S)} \cong \sum_{i=1}^{n_g} g_{Gi} \left(\theta_{Gi} - \theta_{Gi}^S \right)$$

$$+ \sum_{i=1}^{n_g-1} \sum_{j=i+1}^{n_g} V_{Gi} V_{Gj} G_{ij} \left[K_{ij} - T_{ij} \right] \tag{31}$$

where

$$T_{ij} = \theta_{Gi} + \theta_{Gj} - \theta_{Gi}^S - \theta_{Gj}^S . \tag{32}$$

With this approximation, only a few rows of the G matrix are processed. This reduces the computational burden for the dissipation term from the order of n_g^2 to the order of n_g.

3.4 Load Models

The load at any potential load bus will be expressed as:

$$P_{L_i} = P_{L_i}^O \left[A_i \frac{v_i^2}{(v_i^O)^2} + B_i \frac{v_i}{v_i^O} + C_i \right] \tag{33}$$

$$Q_{L_i} = Q_{L_i}^O \left[A_i' \frac{v_i^2}{(v_i^O)^2} + B_i' \frac{v_i}{v_i^O} + C_i' \right] \tag{34}$$

for $i = n_q+1, \ldots, n_T$; and where

$P_{L_i}^O + jQ_{L_i}^O$ = Complex prefault load

v_i^O = Prefault bus voltage magnitude

v_i = Post-fault bus voltage magnitude

A_i, B_i, C_i = Fractions of constant impedance, current, and power, at bus i. Same for primed coefficients.

Obviously, one has the restriction:

$$A_i + B_i + C_i = 1 , \tag{35}$$

and,

$$A_i' + B_i' + C_i' = 1 . \tag{35'}$$

24

Using the Center of Inertia (COI) reference frame, the load flow equations for the post-fault network and for bus $n_g+1,\ldots,n_T$ are given by:

$$P_i = -P_{L_i}(V_i)$$

$$= \sum_{j=1}^{n_T} V_i V_j \left[B_{ij} \sin(\theta_i - \theta_j) + G_{ij} \cos(\theta_i - \theta_j) \right] \tag{36}$$

$$Q_i = -Q_{L_i}(V_i)$$

$$= \sum_{j=1}^{n_T} V_i V_j \left[G_{ij} \sin(\theta_i - \theta_j) - B_{ij} \cos(\theta_i - \theta_j) \right] \tag{37}$$

for $i = n_g+1,\ldots,n_T$. As for the internal generator buses, one has the relation:

$$P_{m_i} = P_{e_i} + \left(\frac{M_i}{M_T}\right) P_{COI}$$

$$= \sum_{j=1}^{n_T} V_i V_j B_{ij} \sin(\theta_i - \theta_j) + \frac{M_i}{M_T} P_{COI} \quad , \quad i = 1,\ldots,n_g-1 \tag{38}$$

$$P_{COI} = \sum_{i=1}^{n_g} (P_{m_i} - P_{e_i}) \tag{39}$$

Finally, one has the restriction:

$$\sum_{i=1}^{n_g} M_{Gi} \theta_{Gi} = 0 \quad , \tag{40}$$

where M_{Gi} is the machine inertia constant associated with generator i. Equations (36)-(40) correspond to those needed for the solution of the Stable and Unstable Equilibrium Points (SEP and UEP, respectively) of the system. With this formulation, the sparse matrix approach can be easily used as explained in more detail in Part 1 of this paper. We note here that in Equation (38) there are no "G_{ij}" terms simply because internal generator resistances can be safely neglected.

3.5 The Transient Energy Function

Using the COI reference frame, the potential energy function, V_{PE}, is given by:

$$V_{PE} = \sum_{i=n+1}^{n_T} \int_{\theta^S}^{\theta} \left[-P_{m_i} + P_{e_i} + \frac{M_i}{M_T} P_{COI} \right] d\phi_i$$

$$= -P_{m_i} \left(\theta_i - \theta_i^S \right) + \sum_{i=n+1}^{n_T} \int_{\theta^S}^{\theta} P_{e_i}(\phi) d\phi_i$$

$$= -P_{m_i} \left(\theta_i - \theta_i^S \right) + \sum_{i=n+1}^{n_T} \sum_{j=1}^{n_T} \int_{\theta^S, V^S}^{\theta, V} V_i V_j B_{ij} \sin(\phi_i - \phi_j) d\phi_i , \qquad (41)$$

where P_{COI} (associated with center of inertia motion) term cancels out, and where

θ^S = vector θ at SEP

ϕ = dummy integration variable.

In Appendix A, we carry out the basic derivation for evaluating the integrals in Equation (41). The resulting expression is given by:

26

$$V_{PE} = -\sum_{i=1}^{n_g} P_{m_i} \left(\theta_i - \theta_i^S \right) - \frac{1}{2} \sum_{i=1}^{n_g} \left[\frac{V_i V_{ti}}{x'_{di}} \cos(\theta_i - \theta_{ti}) - \frac{V_i^S V_{ti}^S}{x'_{di}} \cos\left(\theta_i^S - \theta_{ti}^S\right) \right]$$

$$+ \frac{1}{2} \sum_{i=n+1}^{n_T} \left(Q_i(V_i) - Q_i(V_i^S) \right) + \sum_{i=n+1}^{n_T} Q_{L_i}^O \left[\frac{1}{2} \frac{A_i'}{\left(V_i^O\right)^2} \left(V_i^2 - (V_i^S)^2 \right) \right.$$

$$+ \frac{B_i'}{V_i^O} \left(V_i - V_i^S \right) + C_i' \ln\left(\frac{V_i}{V_i^S}\right) \right] + \sum_{i=n+1}^{n_T} P_{L_i}^O \left[\frac{A_i}{\left(V_i^O\right)^2} \left\{ (V_i^S)^2 \Delta\theta_i + V_i^S \Delta V_i \Delta\theta_i \right. \right.$$

$$\left. + \frac{1}{3} (\Delta V_i)^2 \Delta\theta_i \right\} + \frac{B_i}{V_i^O} \left(V_i^S \Delta\theta_i + \frac{1}{2} \Delta V_i \Delta\theta_i \right) + C_i \Delta\theta_i \right] + \sum_{i=1}^{n_g-1} \sum_{j=1+1}^{n_g} I'_{ij} \,, \qquad (42)$$

where $\Delta\theta_i = \theta_i - \theta_i^S$, $\Delta V_i = V_i - V_i^S$, and

$$I'_{ij} = V_i V_j G'_{ij} \frac{\theta_i + \theta_j - \theta_i^S - \theta_j^S}{(\theta_i - \theta_j) - \left(\theta_i^S - \theta_j^S\right)} \left[\sin(\theta_i - \theta_j) - \sin\left(\theta_i^S - \theta_j^S\right) \right] \,. \qquad (43)$$

G'_{ij} terms correspond to the reduced network (up to internal generator nodes) with all loads set to zero.

This expression for the potential energy function depends explicitly on the various fractional components of the load model and on the reduced conductance matrix representing line conductances only. If line conductances are very small, or negligible, the last summation over I'_{ij} terms can be set to zero and the network reduction process completely avoided. Alternatively, one can restrict that summation to terms where either bus i, or j, or both, correspond to so-called "advanced machines." This is shown to be a very good approximation that reduces the computational burden significantly.

27

3.6 DC Line Model

Appendix C and Ref. [15] describe a procedure for incorporating a DC line model in the classical TEF method. The procedure involves the following steps:

(1) Formulation of DC line equations and dynamics in a form which is simple and adequate for first swing transients analysis.

(2) Since the classical TEF formulation relies on network reduction, the DC terminal buses are retained, together with internal generator nodes.

(3) In the pre-disturbance mode, the simplified DC line model is used in conjunction with the above reduced equations to obtain a prefault solution. This solution provides values of DC line terminal voltages and angles.

(4) In subsequent steps, the DC line model is incorporated into the load flow method for obtaining SEP and UEP solutions.

(5) In order to account for power injections at DC terminal buses, the potential energy expression is correspondingly modified.

(6) Using the modified potential energy function, all TEF analysis is carried out as in the normal classical procedure, but with DC terminal buses represented as constant power injection ones.

In our sparse network formulation with static load models, the DC line model of Appendix C can be accommodated as follows:

(1) Retain the DC line representation but avoid the process of network reduction. For that matter, any efficient load flow program with a DC line model should work.

28

(2) Augment the load flow equations to account for internal generator buses and P_{COI}. These augmented equations should be used for SEP and UEP solutions.

(3) In computing the transient energy function, use the model developed in Section 3.4 assuming that the DC line terminal buses are represented by by an appropriate equivalent load model.

3.7 Excitation System Model

Appendix D provides a detailed description of efforts by Iowa State University (Prof. Fouad and co-workers), under EPRI sponsorship, on excitation system modeling with the classical TEF method. In their estimate, excitation system models will be necessary under certain conditions when the classical model fails to give accurate results.

The approach used consists of the following steps:

(1) Machines with exciter models are reprensented internally by means of the two-axis model.

(2) Theoretically, any exciter model can be represented. However, for high ceiling, high response exciters, a model with one time constant and two cutoff limits on E_{FD} was found adequate for initial evaluation steps.

(3) Because of cutoff limits on E_{FD}, special logics are introduced in the SEP/UEP solution algorithms. In those algorithms, a set of algebraic equations is obtained by setting all time derivatives in the system's differential equations to zero.

(4) The swing equations in the COI reference frame are retained as previously, but with the new exciter variables influencing the P_{e_i} and P_{COI} terms.

29

(5) The MOD is assumed to be known, in advance, basically on the basis of classical models only.

(6) The energy function is rederived using "average" values of E_d' and E_q'.

The results shown in Appendix D are encouraging. They do indicate an increased level of complexity in the solution algorithms. Furthermore, the use of average E_d' and E_q' values will require more scrutiny in large scale tests.

From our vantage point, the derivations in Appendix D can be easily adapted to the sparse matrix formulation. We also have a strong feeling that the derivations used in Section 3.4 and Appendix A will yield an energy function which does not depend on average values of E_d' and E_q'. It is not carried out here because it will entail a significant effort which is beyond the present scope.

3.8 Voltage Conditions at Maximum Swing

In many situations the system will remain within its stabilty limit. However, at maximum swing, some bus voltages will dip below acceptable limits. TEF methodology with sparse matrix formulations provides a natural means for predicting voltage conditions at maximum swing.

Referring back to Section 3.2, the total energy of the system at clearing time is given by:

$$V_{t=tc} = V_{KE,corr} + V_{PE,tc} = V_{KE,corr} + V_{PE}(\theta^C, \theta^S) \ . \tag{44}$$

Let θ^m define the angle vector at maximum swing. At that angle, the corrected kinetic energy [2] will be zero and all energy is strictly potential energy. Consequently, one can write:

$$V_{tc} = V_{KE,corr} + V_{PE}(\theta^c, \theta^s) = V_{PE}(\theta^m, \theta^s) . \qquad (45)$$

Now V_{tc} can be computed exactly at $t = tc$. This means that we have an extra equality constraint to work with. In order to determine θ^m, one makes the usual approximation of a linear trajectory in the angle space from θ^c to θ^u (i.e., UEP). Along that linear trajectory, we determine θ^m such that the above equality constraint is satisfied. A simple search procedure should converge in a few iterations.

In obtaining the voltage at maximum swing, we can outline the following procedure:

(1) Using the sparse matrix formulation (with the desired load model), obtain solutions for $\theta^c, \theta^s, \theta^u$ and $V_{KE,corr}$.

(2) Along the straight line trajectory from θ^c to θ^u, use a search technique to compute θ^m such that Equation (45) is satisfied.

(3) Obtain the voltage $\underline{V}_L^m$ at $\theta = \theta^m$.

(4) Check for voltage dip violations.

3.9 Out-of-Step Relaying

Reference [16] contains a methodology for determining the apparent impedance of a given line at maximum angular swing. As in the previous section, it proposes a similar method for computing θ^m along a linear trajectory from θ^c to θ^u, such that Equation (45) is satisfied. Once this is

achieved, line current and voltages are computed in order to determine its apparent impedance at maximum swing.

Because of the sparse matrix formulation, this task is very easy to achieve. As for the voltage dip case, at $\theta = \theta^m$, we compute $\underline{V}_L^m$ and solve directly for all line apparent impedances. This automatically sets the conditions for out-of-step relay operation.

In this context, the effect of out-of-step relay action may be accounted for. Should a relay operate, then the corresponding switching sequences can be implemented to yield a new set of energy margins.

3.10 Complex Switching Sequences

If one accepts the classical machine model, then a complex switching sequence poses no major problems. There are three alternative approaches:

(1) For every switching interval, use the constant acceleration approximation. This has proven to yield good results, as long as the entire switching sequence is short in duration (e.g., 10-15 cycles).

(2) Use a Taylor series approximation for every switching sequence.

(3) For longer switching intervals, a time domain simulation approach will be necessary. Obviously, this will slow down execution times.

The object here is to obtain θ^c at $t = tc$, which is the last time a switching operation occurs. Following that the normal TEF approach is employed.

32

3.11 Reduced Order Modeling

To be useful to a system operator, a reduced order model of a power system has to retain the same basic form as the original model. That is, it has to be expressable in terms of equivalent generators and transmission lines. In the case of power systems, this has been possible because of the naturally occurring phenomena of coherency. At the same time, the analysis technique used to generate the equivalent should be capable of detecting the structure of the system that causes the coherency. A third and crucial issue is deciding the appropriate level of reduction. As might be expected, the level of reduction depends upon the amount of accuracy desired and the type of disturbance being investigated.

Several methods are available for generating reduced order models that meet some or all of these requirements. The work done for EPRI by Podmore and Germond [19] yields coherency based models, but the method is heuristic and reveals little or nothing about system structure. It is possible, but not practical, to generate a family of equivalents that reflect various degrees of coherency. It is not possible to estimate the proper order of reduction. The reduced order models obtained by this method are "local" in the sense that they are derived for a disturbance at a specific location.

Chow, Kokotovic, Winkelman, et al. [20,21] have used the singular perturbation approach to divide the model of the power system into two subsystems, one consisting of slow oscillations between groups of machines, and the other consisting of higher frequency oscillations occurring within the groups or areas. It is the slow oscillations that are of interest in this case, providing a global picture of how the system responds to major disturbances. This is in contrast to the EPRI approach which concerns itself with particular

33

or "local" disturbances. The actual testing of this system is limited to one study of the WSCC system. There have been no papers by this group of researchers that indicate how to estimate the proper amount of order reduction using this approach.

The model reduction technique used in this report is the modal coherency method initiated by Schlueter [22,23] and extended by Lawler [24,25] and Dorsey [26,27]. As it now stands, this approach is analytically sound, yields the proper kind of physical model, gives a valid estimate of order reduction, can be applied to systems with as many as 2000 generators and 20,000 lines, and is computationally efficient. Figure 3 compares the accuracy of several reduced order models to the unreduced model for a nine cycle fault at Plant Scherer, a major plant connected to the 500 KVA transmission system in the center of the Southern Company System. It is noteworthy that the reduced order models give very accurate results for the first two seconds and are not introduced by each aggregation. It can be seen from the graph that the relative inaccuracies are very small down to aggregation level 200. Thus, a very accurate global model of the system would have about 180 generators. If a slightly less accurate model could be tolerated, it is probably feasible to aggregate down to a 140 generator model. On the other hand, reduced order models of less than 100 generators could not be expected to be very accurate in analyzing interarea oscillations since aggregation will have occurred across relatively weak boundaries.

The graph in Figure 4 was determined by applying appropriate disturbances to all generators in the system [26,27]. Figure 5 shows the order estimation graph for a local disturbance of only generator 269, which is electrically close to the fault under study at bus 1941. Since the disturbance energy is
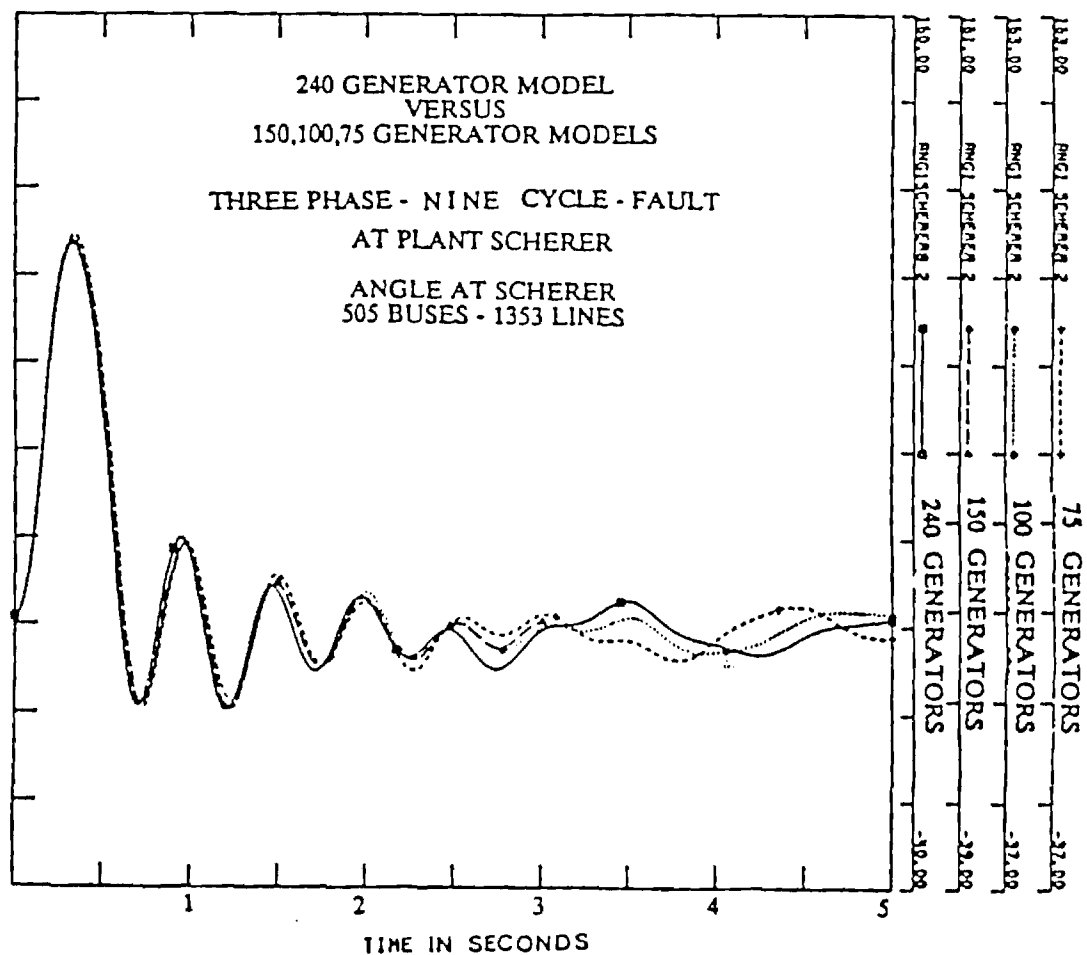
34

Figure 3. Comparison of Time Domain Responses of Detailed and
Reduced Order Models.

WSCC GLOBAL RANKING TABLE
LINE 924 TO 1941 DROPPED
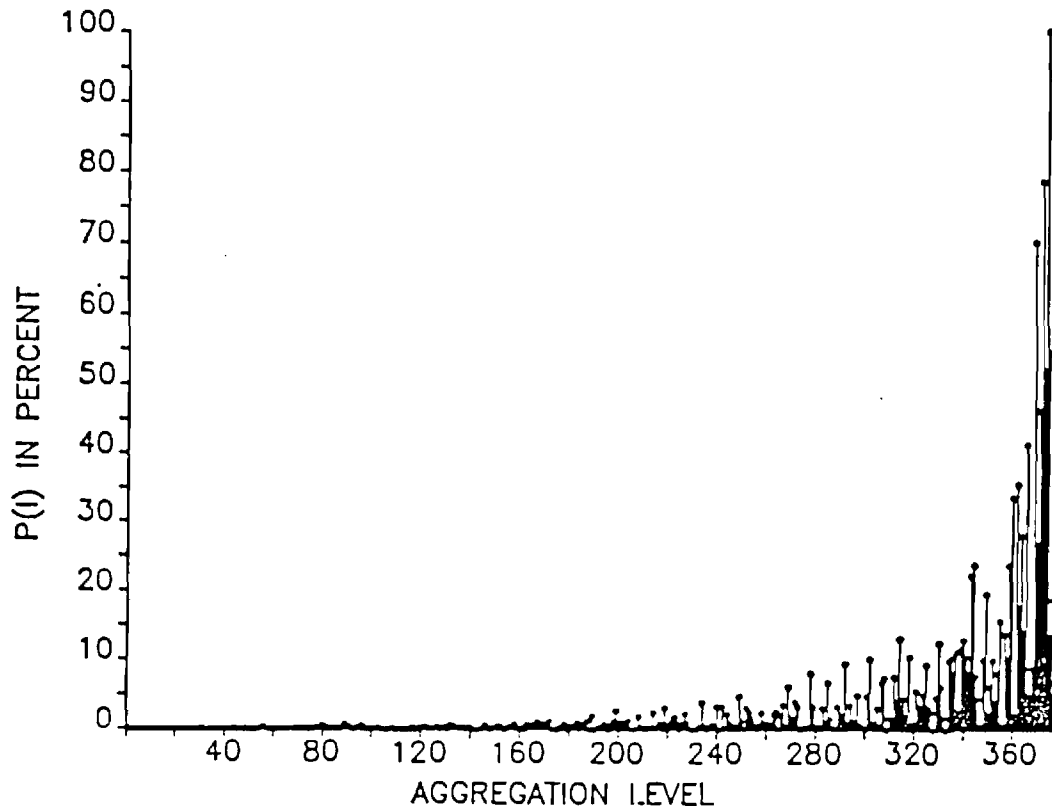SEPTEMBER 11, 1987

Figure 4. Ranking Table for WSCC System.

WSCC ORDER ESTIMATION
DISTURBANCE AT BUS 1307 LINE 924 TO 1941 DROPPED
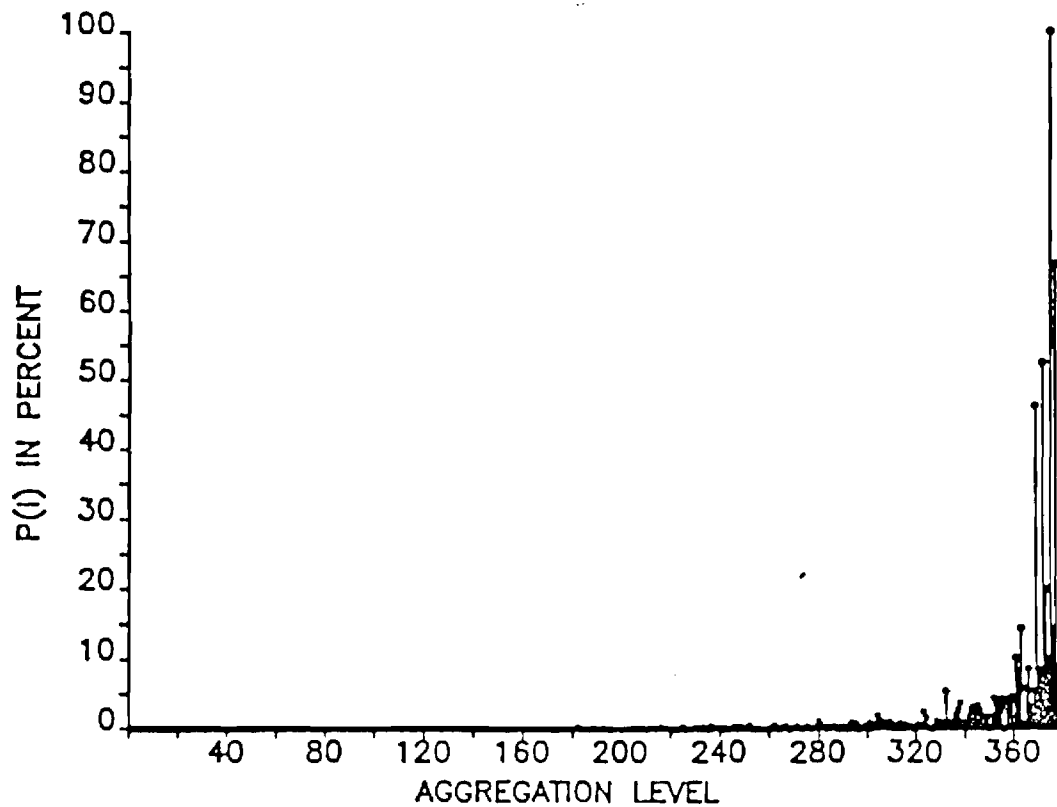SEPTEMBER 11, 1987

Figure 5. Order Estimation for WSCC System.

much more localized in this case, the feasible order reduction is greater, and an accurate result should be achieved with a 50 or 60 generator equivalent. The fact that the feasible amount of aggregation is larger in this case can be explained as follows. Since the disturbance energy is localized, generators electrically distant from the disturbance will be effected to a much smaller extent, and one can expect large groups of these machines to remain coherent. This is a far different situation from the global case where all the machines are disturbed, but the purpose on the global case is different. In the global case, a very robust disturbance is required because the intent is to identify groups of machines that are strongly interconnected. In the case of a local disturbance, the goal is to determine groups of machines that remain coherent in response to a localized disturbance. Whether these machines are tightly interconnected is not the issue, the issue is whether they are coherent in the face of the localized disturbance. One of the significant advantages of the modal coherency method is that it can determine both types of models. Other methods determine one type of model or the other, but not both.

It is also possible to use the local disturbance approach to determine the generators most affected by the disturbance. In the present case, those generators are 155, 156, 205, 269, and 372. This provides a way of determining beforehand the so-called "advanced" machines.

4. TEF FEASIBILITY

4.1 General

Although most past arguments have stressed the role of direct methods in "on-line dynamic security assessment," developments in the last couple of years are generating interest in off-line planning-type studies. In this report, the starting point will focus on the on-line operational component but with strong references to the planning one.

Initially, we shall look at a possible structure of an on-line dynamic security assessment program in light of BPA's technical needs outlined earlier, and the needs of an on-line environment. Feasibility issues then follow. In analyzing these issues, we shall make "intelligent guesses," based on our gained experience, on the levels of confidence in what has been accomplished, and on needed future efforts.

4.2 TEF Operational Structure

In an environment of on-line operation for dynamic security assessment, we envision two complimentary packages: one used in on-line analysis and the other for off-line preparatory and backup studies. The functions of the off-line package are:

(1) Specification of the contingency list including all switching sequences for every contingency.

(2) Specification of the Mode of Disturbance for each contingency.

(3) Ranking of contingencies on basis of transient energy margins and related measures.

(4) Specification of reduced dynamic equivalents for groups of contingencies.

(5) Specifications of model details (e.g., load models, DC line, exciters) needed in the on-line mode.

(6) Determination of approximate operating guidelines for maximum line loadings, inter-area transfers, generation limits, and remedial measures.

(7) Precomputation of sparsity-oriented arrays (network pointers, tables of factors, and some reduced matrices) for later use on the on-line mode.

With these off-line functions, one can specify the on-line functions to consist of:

(1) Calibration of the reduced dynamic equivalents on basis of on-line data collection and exchange.

(2) Fast contingency analysis using the specified MODs and specialized techniques like the ones used in steady-state contingency analysis (e.g., use of the matrix inversion lemma, or network-based sensitivity methods).

(3) Provision of on-line "intelligence" information to the operator in critical cases.

4.3 Computational Effort

Computational efforts associated with the on-line functions consist of the following sequence of computations:

(1) Initial conditions

(2) Conditions at final clearing time

40

(3) SEP

(4) UEP initial vector

(5) UEP

(6) Energy margin analysis.

From a theoretical viewpoint, we shall use the following timing and other parameters to estimate ranges of computational efforts. The following definitions are in order:

T_B = base time unit

= single original network load flow iteration time consisting of Jacobian, mismatch vector, forward and backward substitution

α_1 = n_g/n_t

= ratio of number of generator buses to total number of buses

n_{max} = number of terms in table of factors

α_2 = n_g/n_{max}.

Based on these parameters, we shall make an "expert" guess on needed computational effort:

(1') Initial conditions: $\alpha_2 T_B$

(2') Conditions at final clearing time: $(1.0 + \alpha_2)T_B$

(3') SEP computation: Assuming 5 iterations, one obtains $5(1 + \alpha_1)T_B$

(4') UEP initial vector computation: This typically involves 10 search iterations involving one load flow and one energy function computation: $10(1 + \alpha_2)T_B$

(5') UEP computation: Assuming 10 iterations, one obtains $10(1 + \alpha_1)T_B$

(6') Energy margin analysis: Here we have 3 possible estimates:

(a) Detailed exact computations. This involves $n_g^2/2$ terms, hence, the effort here is given as: $\left(n_g^2/n_{max}\right)T_B$

(b) Approximate computations for constant impedance load model with 5 advanced machines: $5(n_g/n_{max})T_B$

(c) Approximate computations for general load model with 5 advanced machines: $5(n_g/n_{max} + n_T/n_{max})T_B$.

For the WSCC system, the following data is given and/or obtained from actual runs:

$$n_g = 380$$

$$n_T = 2,214 + 380 = 2,594$$

$$n_{max} \cong 15,000$$

Hence,

$$\alpha_1 = .146$$

$$\alpha_2 = .025$$

With this data, and the above estimates, we obtain the following timing information:

T_a = Computation time assuming constant impedance loads and exact energy function computations

$$= (\alpha_2 + 1 + \alpha_2 + 10 + 10 \alpha_2 + 10 + 10 \alpha_1 + n_g\alpha_1)T_B$$

$$= \left(21 + 12 \alpha_2 + (10 + n_g)\alpha_1\right)T_B$$

$$= \underline{78.24\ T_B}$$

T_b = Computation time with constant impedance load model and approximate energy function computations

$$= (21 + 12 \alpha_2 + 15 \alpha_1)T_B$$

$$= 23.49\ T_B$$

T_c = Computation time with general load model and approximate energy function computation

$$= (21 + 12 \alpha_2 + 15 \alpha_1 + n_T/n_{max})T_B$$

$$= 23.66 \ T_B$$

Thus, a single stability case will require, on the average, 23-78 basic load flow iterations for the base case WSCC system. On the Cyber 990 (at Georgia Tech), $T_B \simeq 4$ sec for the WSCC system. For that computer, a typical computation effort requires $(23-78) \times 4 = 92 - 312$ CPU sec.

For purposes of comparison, time domain analysis for a classical machine model for 2 sec simulation time and 1/4 cycle integration step size will require $2 \times 240 \ T_B \simeq 1920$ CPU sec. The improvement factor is $1920/92 -$ $1920/312 \rightarrow 20.8 - 6$ times over time domain simulations. In an actual test of the WSCC 380 generator case, STEF required 92.3 sec of CPU time and time-domain analysis, 226.54 sec. This corresponds to an improvement factor of 2.45. With a non-constant impedance load model, the improvement factor is 58.26.

All of the above estimates assume that:

(1) All pointer arrays for ordered buses are precomputed.

(2) The reduced G-matrix is also available and precomputed.

(3) Base case load flow is exact.

(4) Input/output computation times are not accounted for.

These are reasonable assumptions for an on-line environment. As model complexity increases, the computational effort will also increase. The following are "expert judgements" on increases in computational efforts due to modeling improvements.

4.3.1 Load Models

Incorporation of general load models will increase the number of iterations for SEP and UEP solutions by a factor of two, at the outside. In time domain analysis, the increase is probably three times the original approach.

43

Energy margin computation times will correspond to option (c) above. For the WSCC system, the resulting CPU time estimate for TEF computations is:

$$T_c' = \left(\alpha_2 + 1 + \alpha_2 + 10(1 + \alpha_1) + 10(1 + \alpha_2)\right.$$

$$\left. + 20(1 + \alpha_1) + (5\alpha_2 + \frac{n_T}{n_{max}}))\right)T_B$$

$$= (41 + 17\,\alpha_2 + 30\,\alpha_1 + \frac{n_T}{n_{max}})T_B$$

For time domain computations based on the above assumptions, the CPU time estimate is:

$$T_t = 2 \times 240 \times 3\ T_B$$

$$= 1440\ T_B$$

The resulting improvement factor is:

$$\frac{T_t}{T_c'} = \frac{1440}{\left(41 + 17\,\alpha_2 + 30\,\alpha_1 + \frac{n_T}{n_{max}}\right)}$$

For the base case WSCC system, this factor is 31.3. In effect, a detailed load model will tend to penalize time domain analysis more heavily than TEF analysis. The rationale is that for a constant impedance load, the network equations in time domain analysis, are linear. With a detailed load model, they become nonlinear requiring an average of 3 iterations per solution. In TEF, the SEP and UEP equations are nonlinear, regardless of the choice of the load model.

44

4.3.2 DC Line Models

Since the inclusion of DC line models influences load flow solution times, one would expect estimates favoring TEF analysis. A conservative estimate would be of the same order of the inclusion of detailed load models.

4.3.3 Excitation System Models

In time domain analysis, the inclusion of exciter models increases the computational effort by a minor amount. Basically, most of the CPU time is spent on load flow analysis, and not in the integration equation. With the use of exciters with very small time constants, the integration step size will have to be reduced. As a result, there may be a serious increase in CPU times.

In TEF analysis with exciter models, the size of the resulting load flow problem (for SEP and UEP computations) will increase in the number of variables (at least two extra variables per machine with exciter models). There will also be an increase in the complexity of the computational algorithms involved.

Our estimate is that the overall improvement ratio of TEF over time domain analysis will remain within the bounds discussed above.

4.3.4 Voltage Condition at Maximum Swing/Out-of-Step Relaying

Computation of voltage condition and apparent impedances at maximum swing will require an extra search along the ray line from θ^c to θ^u. Computational effort for that is of the same order as that for obtaining the initial UEP solution, given by:

$$10(1 + \alpha_2)T_B \; .$$

This is effectively ten extra load flow iterations.

45

4.3.5 Multiple Switching Cases

The worst situation in multiple switching cases is to perform time domain simulations during the switching sequence in order to obtain θ^c. This will put TEF on an equal par with time domain analysis during the switching sequence period. Assuming an average case where the switching sequence will last 15 cycles, there will be an extra

$$15 \times 4 \times 2 \; T_B = 120 \; T_B$$

One can improve on this extra burden by using the constant acceleration approximation between any two switchings. For a five switching sequence, the resulting effort is:

$$5(1 + \alpha_2)T_B \; ,$$

which is a considerable improvement. In the worst case, the TEF-over-time domain improvement ratio will become 3.4-2.4 as compared with 20.8-6.0 shown earlier for the WSCC system. The use of the constant acceleration approximation between switchings will change the improvement ratios to 16.5-5.8.

4.3.6 Dyanmic Reduction

Given the present status of dynamic coherency reduction as outlined earlier in this report, there is a tradeoff between the level of reduction and corresponding CPU computational times for both TEF and time-domain analysis. There is obviously a parallel tradeoff in the accuracy of solutions. The computational tradeoff occurs because as machines are aggregated into equivalent ones, the density of nonzero terms in the reduced system's matrix and table of factors changes. Initially, at lower levels of aggregation, the size

46

of the table of factors decreases. At some aggregation level, it levels off and then starts to increase. Table 1 shows this tradeoff for the WSCC system. At some aggregation level, it becomes advantageous to perform complete network reduction to internal generator nodes. We suspect, however, that at such an aggregation level the accuracy of results may be suspect.

4.4 Computational Results

4.4.1 General

In this section, results for studies on three basic systems are described. The purpose of the studies is aimed at illustrating:

(1) Validity and level of accuracy in predicting stability and instability with the basic TEF formulation

(2) Accuracy of developed load models

(3) Impact of network reduction on accuracy of results

(4) Convergence/divergence issues.

The three systems tested are:

(1) 9-bus, 3-generator system (Figure 6)

(2) 39-bus, 10-generator system (Figure 7)

(3) 2214-bus, 380-generator system WSCC system (data provided by BPA).

4.4.2 Basic Verification

9-Bus System: For the 9-bus system, a fault is applied at bus 7 and then cleared by removing line (5-7). Time domain analysis verified that T_c, the critical clearing time is ≈ 9.75 cycles. In Table 2, we show the basic energy parameters at $T_c = 9.75$ cycles. The energy margin at this clearing time is slightly positive. It becomes negative at $T_c = 10.25$ cycles. The breakdown of the potential energy components at UEP is as follows:

47

Table 1. Numbers of Non-Zero Terms in Tables of Factors as
Generators are Aggregated in Coherency Reduction

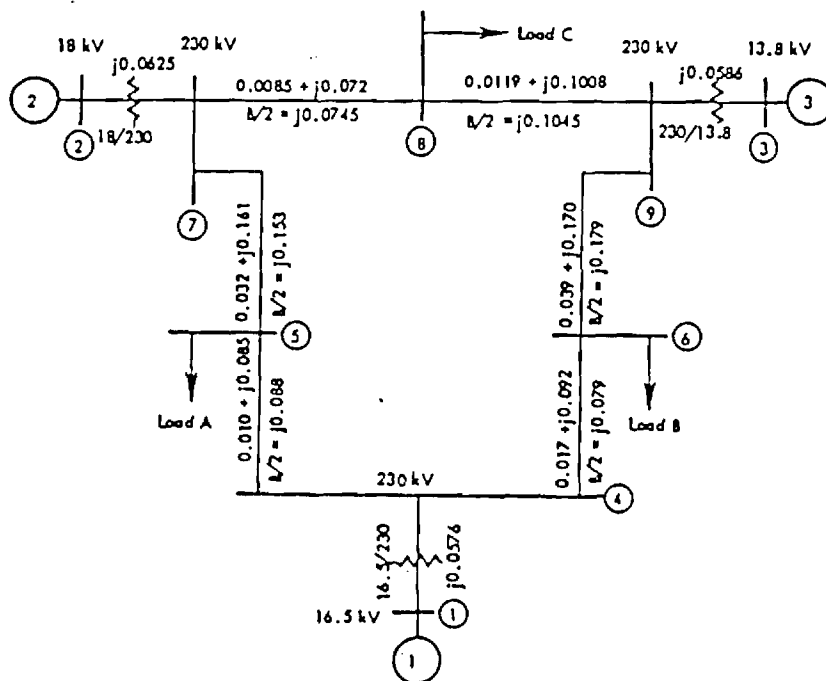| Number of Generators	Size of Load Flow TOF*	Size of SEP/UEP TOF*
380	15666	17527
208	16139	17521
198	15982	17325
60	23126	21500

*Table of Factors

Figure 6. 9-Bus System Used in Study. (Source:
Book by Anderson and Fouad entitled,
"Power System Control and Stability,"
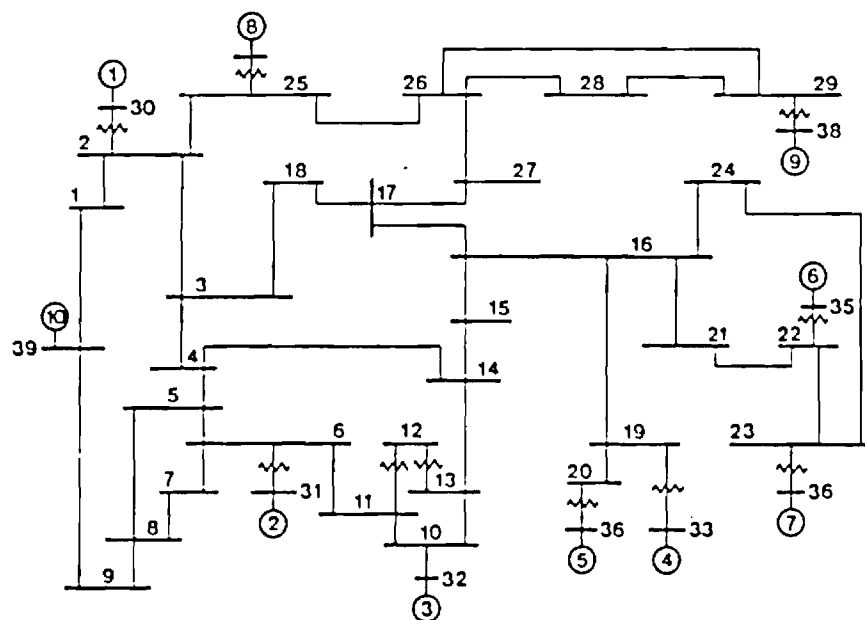Iowa State University Press, Ames, IA)

Figure 7. 39-Bus System Used in Study.

Table 2. Key Transient Energy Parameters for
9–Bus System at T_C = 9.75 cycles

Energy Margin	Normalized Energy Margin	Kinetic Energy	Corrected Kinetic Energy
.0552	.0673	.8707	.8204

P_m term	:	-2.928
Magnetic term	:	3.0656
Overall G-matrix term	:	0.7615

In Table 3, the SEP and UEP solutions are shown. In Table 4, the voltages and angles at all network buses at SEP and UEP are also shown. From Table 3, one notes that the "mode of disturbance" consists of machines 2 and 3 going unstable. The voltages at UEP (Table 4) show a general collapse of significant proportions.

The above results illustrate a key advantage of this approach whereby network solutions are a naturally important by-product.

39-Bus System

Turning to the 39-bus system, we applied a fault at bus 26 which is cleared by removing line 26-27. As shown in Figure 8, time domain analysis demonstrates that instability occurs for a clearing time T_c between 8 and 8.25 cycles, with machine no. 9 breaking away from the rest of the system. TEF analysis confirms this mode of disturbance. In Table 5, we show the breakdown of energy function components for both the exact and approximate G-matrix terms. Table 6 provides values of the SEP and UEP solutions. Finally, Table 7 provides voltage and angle values of selected network buses at SEP and UEP to illustrate the level of voltage collapse at the UEP.

The breakdown of the potential energy at UEP is as follows:

P_m term	:	-15.8943
Magnetic energy term	:	11.6299
G-matrix term (exact method)	:	6.4856
G-matrix term (approximate method)	:	6.7633

This illustrates the good degree of approximation associated with the G-matrix terms.

Table 3. SEP and UEP Solutions of 9-Bus Case

Machine Number	Terminal Bus	SEP (Degrees)	UEP (Degrees)
1	1	-10.49	-41.03
2	2	31.22	110.72
3	3	16.02	86.79

Table 4. Network Solutions at SEP
and UEP for 9-Bus Case

Bus Number	SEP		UEP	
	Voltage	Angle	Voltage	Angle
1	1.0125	-12.19	.8418	-40.05
2	1.0043	20.90	.8494	100.13
3	.9929	7.51	.6689	75.63
4	.9717	-13.94	.6388	-38.51
5	.9228	-19.55	.6066	-44.12
6	.9499	-10.32	.3888	-14.23
7	.9944	15.24	.7608	92.53
8	.9763	8.6	.6587	82.21
9	.9895	4.69	.5659	69.17

Table 5. Breakdown of Various Transient Energy
Terms for Both the Exact and Approximate
G-Matrix Terms, for the 39-Bus System

Solution Method	Energy Margin	Normalized Energy Margin	Kinetic Energy	Corrected Kinetic Energy
Exact	-.1588	-.076	3.4792	2.0892
Approximate G-Matrix Term	-.0574	-.0275	3.4792	2.0892
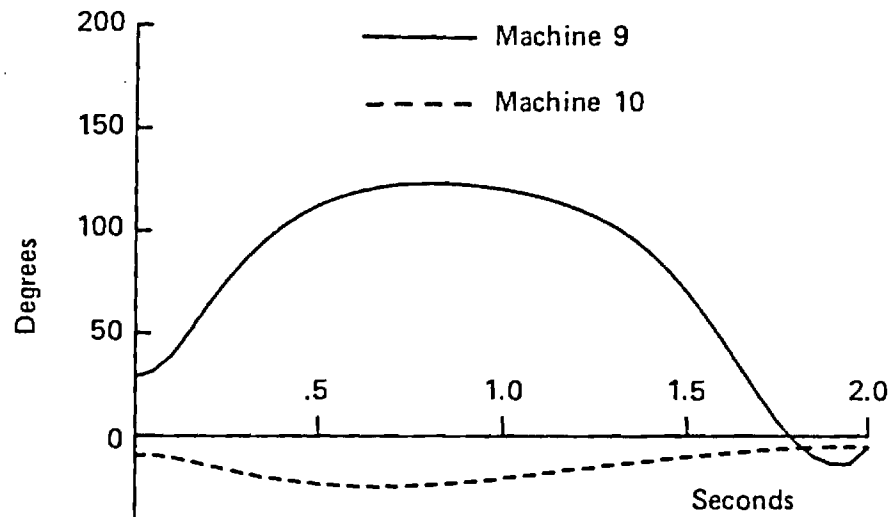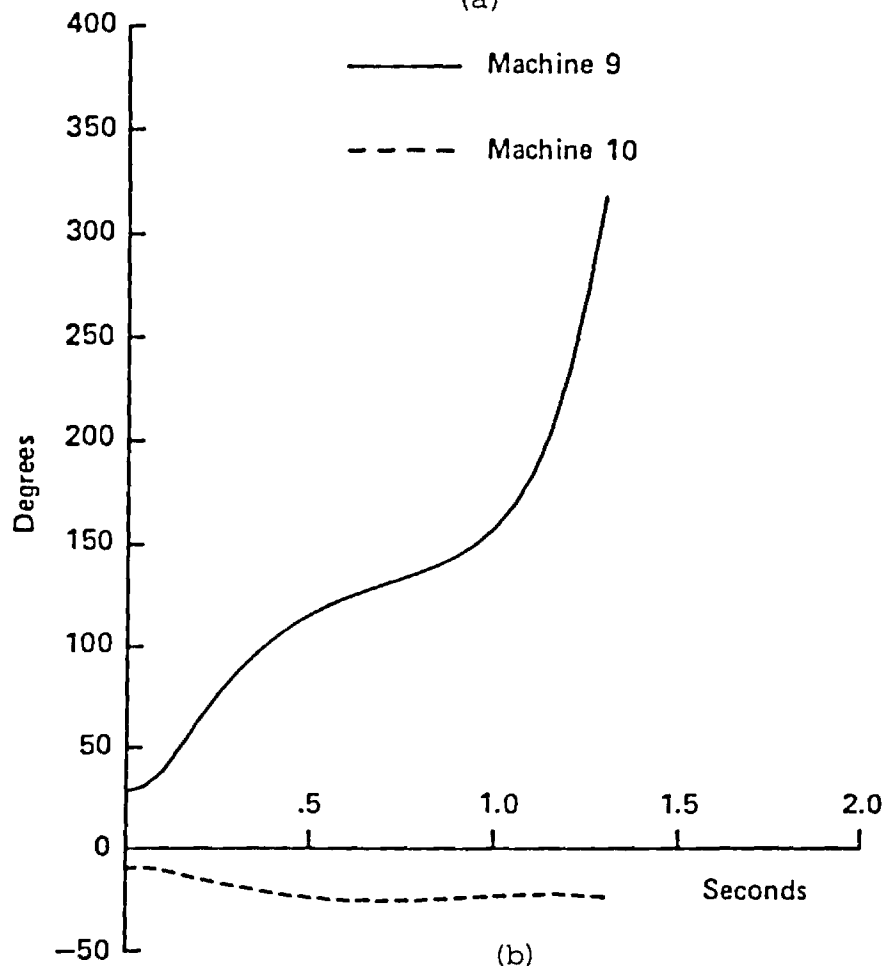
Figure 8. Time Domain Responses of Machines 9 and 10 for 39-Bus System, (a) 8 Cycles Fault, and (b) 8.25 Cycles Fault.

54

Table 6. Stable and Unstable Equilibrium Point
Solutions for the 39-Bus System (Note:
Machine 9 is the only advanced one)

Machine Number	Terminal Bus	SEP (Degrees)	UEP (Degrees)
1	30	-1.04	5.18
2	31	17.42	19.66
3	32	17.40	20.17
4	33	14.22	18.86
5	34	26.43	30.39
6	35	16.46	20.97
7	36	17.17	21.81
8	37	17.58	34.44
9	38	32.76	124.29
10	39	-9.57	-18.59

Table 7. SEP and UEP Solutions at Selected
Network Buses for the 39-Bus System

Bus Number	SEP		UEP	
	Voltage	Angle	Voltage	Angle
25	1.0696	-5.1	.8767	7.99
26	1.0877	-2.75	.6595	26.87
27	.9986	-14.77	.9292	-9.93
28	1.0809	.19	.5674	49.96
29	1.0789	2.78	.5629	60.06
30	1.0444	-4.88	.9441	1.72
31	.9767	-2.13	.9382	.53
37	1.0366	1.53	.8984	16.79
38	1.05	9.49	.5890	82.05

WSCC System

A limited amount of testing of the WSCC system was performed. The 1986 380 generator case was run for a fault condition in the BPA part of the system. A critical fault of 11.7 cycles was applied at bus 1015 with line 1015-1039 cleared. Time domain analysis confirmed a critical clearing time of 12 cycles. This was difficult to do because some low inertia machines, mainly synchronous condensers, were causing some numerical problems. Small integration steps were necessary to insure numerical stability.

With a constant impedance load model, the following results were obtained:

$$\text{Normalized Energy Margin} = .0485$$

$$\text{Position Energy} = -30.376$$

$$\text{Magnetic Energy} = 37.146$$

$$\text{Dissipation Energy} = -3.3623$$

These indices were based on the automatically selected Mode of Disturbance (MOD) of generators Nos. 118 and 119. The complete solution associated with this case is given in Appendix E.

4.4.3 Load Model Results

For the 9-bus system, the applied fault is at bus 7 with clearance of line 7-5 at clearing time. From time domain simulations, one obtains critical clearing times for three different load model configurations as shown in Table 8. At these clearing times, one obtains the energy margins shown in Table 9. All of the margins are close to zero indicating the correctness of the derived energy functions. In that table, dissipation energies at corresponding UEPs are broken down into terms associated with load and line conductances, respectively. As one looks at Table 10, one car arrive at the

56

Table 8. Case Specification and Corresponding
Critical Clearing Times Obtained from
Time-Domain Simulations for the 9-Bus
Test System

Case Number	Load Model			Critical Clearing Time
	Constant Y	Constant I	Constant P	
1	1.0	0.0	0.0	9.75 cycles
2	0.5	0.5	0.0	9.00 cycles
3	0.7	0.0	0.3	8.00 cycles

Table 9. Breakdown of Energy Components of Cases
in Table 1 at Corresponding Critical
Clearing Times (Dissipation Energies are
at Corresponding UEPs)

Case Number	Energy Margin	Normalized Energy Margin	Load Dissipation Energy	Line Conductance Dissipation Energy
1	-.0139	-.017	.4934	.1848
2	.0083	.0119	.3024	.1695
3	-.0073	-.011	.1224	.1542

Table 10. Selected Components of Potential Energy
at UEP for the Cases in Table 1

Case Number	P_m Term	Magnetic Energy
1	-2.9298	3.0656
2	-2.7986	3.0823
3	-2.6448	3.0822

important preliminary conclusion that the critical clearing time is quite sensitive to load model representation as depicted in the load dissipation energy terms.

In a similar fashion, Table 11 defines the various cases and corresponding critical clearing times for the 39-bus system with fault at bus 26 which is cleared by removing line 26-27. In that table, "original method" refers to that used in Part 1 without G-matrix terms approximations. The "new method" refers to the one described here without any approximations. Finally, the method with G-matrix approximations refers to present load modeling, but where G-matrix terms are approximated.

Results of these cases are shown in Table 12. As expected, the energy margins are small pointing to the accuracy of the approaches used. The interesting results are associated with the dissipation energy terms. It is obvious that sensitivity to load dissipation is quite significant.

As for the WSCC system, two cases with the same fault conditions previously stated and MOD were tested. They correspond to (1) 70% constant impedance and 30% constant current load and (2) 90% constant impedance and 10% constant power load. Summary results for these cases are:

Case (1)

Normalized Energy Margin = -.0567

Potential Energy Margin = 3.0

Case (2)

Normalized Energy Margin = -.1082

Potential Energy Margin = 2.828

The details of both cases are given in Appendices F and G. These preliminary results indicate that the introduction of constant current and/or

Table 11. Specification of Load Models, Critical Clearing
Clearing Times and Energy Function Evaluation
Approach for 39-bus System Tests

Case Number	Load Model Constant Y	Constant I	Constant P	Critical Clearing Time	Comment
1	1.0	0.0	0.0	8.0 cycles	Original Method
2	1.0	0.0	0.0	8.0 cylces	New Method
3	0.0	1.0	0.0	7.5 cycles	New Method
4	0.0	1.0	0.0	7.5 cycles	New Method Approx. G Terms
5	0.7	0.0	0.3	8.0 cycles	New Method
6	0.7	0.0	0.3	8.0 cycles	New Method Approx. G Terms

Table 12. Breakdown of Various Energy Terms
at Critical Clearing Times for
the Case Specified in Table 4

Case Number	Energy Margin	Normalized Energy Margin	Load Dissipation Energy	Line Conductance Dissipation Energy
1	-.1588	-.076	0.0	6.4856*
2	-.1269	-.0647	5.2243	1.0247
3	-.0604	-.0392	1.6633	.8425
4	-.0073	-.0047	1.6633	.9222
5	-.0076	-.0049	2.7061	.8891
6	.041	.026	2.7061	.9682

*This term combines load and line conductance dissipations.

constant power components will tend to reduce the margin of stability. Or in other words, the sensitivity to load model parameters is quite significant.

4.4.4 Dynamic Reduction

In the area of dynamic reduction, only the 39-bus and WSCC systems were considered.

For the 39-bus system, the global reduction approach was used to reduce the number of generators from ten to six. The six generators correspond to the following aggregates: (1,4,8), (2,3), (5), (6,7), (9), and (10). For the fault on bus 26, which is central to the system, the following cases were analyzed:

Case 1: Standard TEF

Case 2: Standard TEF with approximate energy formula

Case 3: Structure preserving model

Case 4: Structure preserving model with approximate energy formula.

In all cases, the constant impedance model was used. Table 13 provides basic results for all these cases with t_c = 8 cycles, which is the actual critical clearing time.

As for the WSCC system, a 200 generator and a 60 generator reduced models were tested. The models were obtained on the basis of a fault on bus 1015. Results for these two cases are given in detail in Appendices H and I. In discussing these results, we note the following: For the 200 generator model, the normalized energy margin is .7365. As we go to the 60 generator model, this margin is 1.59. Thus, there is a tendency for the energy margin to increase as the level of aggregation also increases. Our guess is that some machines, which are close to those in the MOD, have to be aggregated, causing this inaccuracy to occur. In fact, for the 60 generator model, one of the

original machines in the MOD was aggregated out with other machines. In effect, we can conclude that what is needed is an aggregated model which preserves all machines in the study area and in all neighboring areas in the vicinity of the fault. Since the present software did not permit this possibility, the severe aggregation levels obtained gave an incorrect stability assessment.

**Table 13.   Results for Reduced 39-Bus System for
Same Fault Conditions Discussed Earlier**

Case Number	Normalized Energy Margin	Overall Dissipation Energy
1	.0126	7.146
2	.0594	7.375
3	-.0725	6.8163
4	-.0574	6.84

5. CONCLUSIONS AND RECOMMENDATIONS

5.1 Conclusions

The main conclusions of the feasibility study are:

(1) For an on-line environment, TEF is computationally more efficient than time domain analysis within one to two orders of magnitude improvements in computational CPU times for large scale system applications. The improvements are more pronounced in those cases where non-constant impedance load models are used.

(2) Upgrading of the present software to incorporate:

   (a) Multiple switching sequences

   (b) Voltage dips at maximum swing

   (c) Out-of-step relay computations are within reach, posing no serious conceptual problems.

(3) The incorporation of the DC line model can be done, in principle, posing, again, no serious conceptual problems.

(4) Incorporation of exciter system models can be accomplished. However, some detailed testing with the EPRI methodology is still needed to reach some conclusions.

(5) Coherency-based reduced-order models can be easily tested with the developed software. Detailed assessments of energy margins using reduced-order models are still required.

5.2 Recommendations

Because of the developmental initiative undertaker in this project to provide a definitive assessment of BPA's needs, there is a need for two future activities:

63

(1) In the first activity, conclusions (2) and (5) above should be implemented as an extension of the present effort in the STEF software package and then a thorough series of detailed tests carried out. Such an activity can be implemented with little additional effort.

(2) In the second activity, the DC line and exciter system models can be implemented. It is suggested that, for the DC line case, both EPRI's and BPA's models be examined to arrive at agreements in results. As for the exciter models, some additional research will be needed, together with detailed testing and evaluation.

REFERENCES

[1] "Direct Analysis of Transient Stability for Large Power Systems," Final Report EPRI EL-4980, Project 2206-1, prepared for EPRI by Ontario Hydro, Toronto, Canada, December 1986.

[2] IEEE Committee Report, Anjan Bose, Chairman, "Application of Direct Methods to Transient Stability Analysis of Power Systems," IEEE Trans. on Power Apparatus and Systems, vol. PAS-103, pp. 1628-1636, 1984.

[3] A. A. Fouad and S. E. Stanton, "Transient Stability of Multimachine Power System, Parts I and II," IEEE Trans. on Power Apparatus and Systems, vol. PAS-100, pp. 3408-3424, July 1981.

[4] A. A. Fouad, et al., "Transient Stability Margin as a Tool for Dynamic Security Assessment," EPRI Report No. EL-1755, March 1981.

[5] A. N. Michel, A. A. Fouad, and V. Vittal, "Power System Transient Stability Using Individual Machine Energy Functions," IEEE Trans. Circuits and Systems, vol. CAS-30, pp. 266-276, 1983.

[6] David Hill and Chong Chi Nai, "Energy Functions for Power Systems Based on Structure Preserving Models," Proc. 25th Conf. on Decision and Control, Athens, Greece, pp. 1218-1223, December 1986.

[7] Bergen and D. J. Hill, "A Structure Preserving Model for Power System Stability Analysis," IEEE Trans. Power Apparatus and Systems, vol. PAS-100, no. 1, pp. 25-35, January 1981.

[8] T. Athay, R. Podmore, and S. Virmani, "A Practical Method for Direct Analysis of Transient Stability," IEEE Trans. Power Apparatus and Systems, vol. PAS-98, pp. 573-580, 1979.

[9] T. Athay, et al., "Transient Energy Analysis," System Engineering for Power, Emergency Operating State Control, Section IV, U.S. Dept. of Energy, Publication No. CONF-790904-PI.

[10] A. H. El-Abiad and K. Nagappan, "Transient Stability Regions of Multimachine Power Systems," IEEE Trans. Power Apparatus and Systems, vol. PAS-85, no. 2, pp. 169-178, February 1966.

[11] M. Ribbens-Pavella, B. Lemal, and W. Pirard, "On-Line Operation of Lyapunov Criterion for Transient Stability Studies," Proc. IFAC Symp., Melbourne, Australia, pp. 292-296, 1977.

[12] J. L. Willems, "Direct Methods for Transient Stability Studies in Power System Analysis," IEEE Trans. Automatic Control, vol. AC-16, no. 4, pp. 232-241, August 1971.

[13] P. Varaiya, F. F. Wu, and R.-L. Chen, "Direct Methods for Transient Stability Analysis of Power Systems: Recent Results," Proc. of the IEEE, vol. 73, no. 13, pp. 1703-1715, December 1985.

[14] A. A. Fouad, et al., "Direct Transient Stability Analysis Using Energy
      Functions: Application to Large Power Networks," Paper No. 86 WM 066-5,
      presented at the IEEE-PES Winter Meeting, New York, New York, February
      1986.

[15] Y. X. Ni and A. A. Fouad, "A Simplified Two-Terminal HVDC Model and Its
      Use in Direct Transient Stability Assessment," Paper No. WP87-96,
      presented at the 1987 IEEE Winter Power Meeting, New Orleans, Louisiana,
      February 1987.

[16] V. Vittal, T. Oh, and A. A. Fouad, "Correlation of the Transient Energy
      Margin to the Out-of-Step Impedance Relay Operation," presented at the
      1987 IEEE Winter Power Meeting, New Orleans, Louisiana, February 1987.

[17] A. Debs, I. Belmona, and T. Godart, "TEF Direct Stability Analysis, Part
      1:   Sparse Matrix Formulation," submitted for presentation at the 1988
      IEEE Winter Power Meeting.

[18] A. Debs, I. Balmona, and T. Godart, "TEF Direct Stability Analysis, Part
      2:   Static Load Models," submitted for presentation at the 1988 IEEE
      Winter Power Meeting.

[19] R. Podmore and A. Germond, "Development of Dynamic Equivalents for
      Transient Stability Studies," Final Report on EPRI Research Project 763,
      April 1977.

[20] B. Aramovic, P. V. Kokotovic, J. R. Winkelman, and J. H. Chow, "Area
      Decomposition for Electromechanical Models of Power Systems," IFAC
      Symposium on Large Scale Systems: Theory and Applications, Toulouse,
      France.

[21] J. H. Chow, J. J. Allemong, and P. V. Kokotovic, "Singular Perturbation
      Analysis of Systems with Sustained High Frequency Oscillations,"
      Automatica, vol. 14, 1978.

[22] R. A. Schlueter, H. Akhtar, and H. Modir, "An RMS Coherency Measure: A
      Basis for Unification of Coherency and Modal Analysis Model Aggregation
      Techniques," 1978 PES Summer Power Meeting.

[23] R. A. Schlueter, U. Ahn, and H. Modir, "Modal Analysis Equivalents
      Derived Based on the R.M.S. Coherency Measure," IEEE Trans. on Power
      Apparatus and Systems, vol. PAS-98, no. 1143, July/August 1979
      (abstract) of 1979 PES Winter Power Meeting, paper no. 79 CH 1418-C.

[24] J. Lawler, R. Schlueter, P. Rusche, and D. L. Hackett, "Modal-Coherent
      Equivalents Derived from an R.M.S. Coherency Measure," IEEE Trans. on
      Power Apparatus and Systems, vol. PAS-99, no. 4, pp. 1415-1425,
      July/August 1980.

[25] J. Lawler and R. Schlueter, "Computational Algorithms for Constructing
      Modal-Coherent Dynamic Equivalents," IEEE Trans. on Power Apparatus and
      Systems, vol. PAS-101, pp. 1070-1080, May 1972.

[26] J. Dorsey and R. A. Schlueter, "Global and Local Dynamic Equivalents Based on Structural Archetypes for Coherency," IEEE Trans. on Power Apparatus and Systems, vol. PAS-102, pp. 1793-1801, June 1983.

[27] J. Dorsey and R. A. Schlueter, "Structural Archetypes for Coherency: A Framework for Comparing Power System Equivalents," Automatica, vol. 20, no. 3, pp. 349-353, May 1984.

[28] G. Troullinos and J. Dorsey, "Application of Balanced Realizations to Power System Dynamic Equivalents," IEEE Trans. on Automatic Control, vol. AC-30, no. 4, pp. 414-416, April 1985.

[29] G. Troullinos, J. Dorsey, H. Wong, J. Myers, and S. Goodwin, "Estimating Order Reduction for Power System Dynamic Equivalents," IEEE Trans. Power Apparatus and Systems, vol. PAS-104, no. 12, pp. 3475-3481, December 1985.

[30] G. Troullinos, J. Dorsey, H. Wong, and J. Myers, "Reducing the Order of Very Large Power System Models," IEEE-PES Winter Power Meeting, paper no. 87 WM 097-9, February 1-6, 1987.